Transportation Research Part E 172 (2023) 103085

Contents lists available at ScienceDirect

Transportation Research Part E

journal homepage: www.elsevier.com/locate/tre

A comparative analysis of charging strategies for battery electric buses in wholesale electricity and ancillary services markets[☆]

Nico Brinkel[a,*,1], Marle Zijlstra[a,1], Ronald van Bezu[b], Tim van Twuijver[b], Ioannis Lampropoulos[a], Wilfried van Sark[a]

[a] Copernicus Institute of Sustainable Development, Utrecht University, Princetonlaan 8a, 3584 CB, Utrecht, The Netherlands
[b] Qbuzz B.V., Piet Mondriaanplein 31, 3812 GZ, Amersfoort, The Netherlands

ARTICLE INFO

Keywords:
Battery electric buses
Smart charging
V2G
Ancillary services
Grid impact analysis

ABSTRACT

The application of smart charging to battery electric buses can provide opportunities for bus operators to reduce the operational costs of their bus fleet. This research aims to create insight into the impact of different charging strategies for battery electric bus fleets on charging costs and the grid load. It proposes a novel framework to model the charging process of battery electric buses for different charging strategies: charging-on-arrival, peak-shaving, day-ahead market optimization with and without vehicle-to-grid (V2G) functions, including the provision of Frequency Containment Reserves (FCR) and automatic Frequency Restoration Reserves (aFRR) for system balancing in ancillary services markets. Model simulations are conducted to compare the charging costs and grid impact of different charging strategies, using three depots of bus operator Qbuzz in the Netherlands as a case study. Results indicate that the application of smart charging algorithms can considerably reduce charging costs for bus operators. Application of the peak-shaving strategy was found to reduce charging costs by 23–32% compared to the reference case of charging-on-arrival. Charging costs can be further reduced by 6–11% when considering day-ahead market optimization. Participation in ancillary services markets for system balancing is economically attractive for bus operators, particularly in the aFRR market, characterized by a cost reduction potential of 90–>100% compared to the charging-on-arrival strategy. The grid impact analysis indicates that charging-on-arrival can result in high charging demand peaks, which can be drastically reduced by the application of peak-shaving or day-ahead market optimization charging strategies. However, the provision of aFRR and FCR using the battery electric bus charging process can have a severe impact on the local grid in terms of high peak demand.

1. Introduction

Road transport is one of the major contributors to global greenhouse gas (GHG) emissions and is thus a main driver of anthropogenic global warming. In 2018, around 20% of the European GHG emissions originated from road transport

☆ This research is a result of the Integrated and Replicable Solutions for Co-Creation in Sustainable Cities (IRIS) project, which received funding from the EU Horizon 2020 research and innovation program under grant agreement No. 774199. In addition, this project is supported by the Dutch Ministry of Economic Affairs and Climate Policy and the Dutch Ministry of the Interior and Kingdom Relations through the ROBUST project under grant agreement MOOI32014.

* Corresponding author.
E-mail address: n.b.g.brinkel@uu.nl (N. Brinkel).

[1] Equal contributions.

https://doi.org/10.1016/j.tre.2023.103085
Received 10 June 2022; Received in revised form 23 January 2023; Accepted 26 February 2023
Available online 10 March 2023

Nomenclature

Indices and sets

$i \in \mathcal{I}$	Set of FCR auctions in the assessment timeframe.
$s \in \mathcal{S}$	Set of charging transactions.
$t \in \mathcal{T}$	Set of time steps in the assessment timeframe.

Variables - Charging strategies

C	Overall charging costs [€].
$\mathrm{C}_{\mathrm{deg}}$	Battery degradation costs [€].
$\mathrm{P}_{\mathrm{ch,tot},t}$	Total charging power at time t [kW].
$\mathrm{P}_{\mathrm{ch},t,s}$	Charging power of transaction s at time t [kW].
$\mathrm{P}_{\mathrm{disch,tot},t}$	Total discharging power at time t [kW].
$\mathrm{P}_{\mathrm{disch},t,s}$	Discharging power of transaction s at time t [kW].
$\mathrm{P}_{\mathrm{peak}}$	Peak net total charging power during the assessment timeframe [kW].
$\mathrm{SoC}_{t,s}$	Battery SoC at the beginning of time t of transaction s [%].

Variables - Ancillary service models

$\mathrm{P}_{\mathrm{FCR\ accepted\ bid},i}$	Accepted FCR bid in auction i [kW].
$\mathrm{P}_{\mathrm{FCR/aFRR\ (up/down)\ activated},t}$	Activated FCR/aFRR upward/downward power at time t [kW].
$\mathrm{P}_{\mathrm{FCR/aFRR\ (up/down)\ fleet\ max},t}$	Max. FCR/aFRR upward/downward bid at time t [kW].
$\mathrm{P}_{\mathrm{FCR/aFRR\ bid\ (up/down)}}$	Upward/downward FCR/aFRR bid size [kW].
$\mathrm{P}_{\mathrm{FCR/aFRR\ grid\ max}}$	Max. upward/downward FCR/aFRR power without exceeding $\mathrm{P}_{\mathrm{peak,max}}$ [kW].
$\mathrm{P}_{\mathrm{FCR/aFRR\ up/down\ fleet\ max},t}$	Max. upward/downward FCR/aFRR power that can be provided at time t [kW].
$\mathrm{P}_{\mathrm{FCR/aFRR\ up/down\ max},t,s}$	Max. upward/downward FCR/aFRR power that can be provided at time t by transaction s [kW].

Parameters

$\Delta \mathrm{f}_{\mathrm{full}}$	Frequency deviation with full bid activation [Hz].
$\Delta \mathrm{f}_{\mathrm{min}}$	Min. frequency deviation for FCR activation [Hz].
$\Delta \mathrm{t}$	Time step duration [h].
η_{ch}	Charging efficiency [%].
η_{disch}	Discharging efficiency [%].
$\pi_{\mathrm{aFRR\ bid\ down}}$	Downward aFRR bid price [€/kWh].
$\pi_{\mathrm{aFRR\ bid\ up}}$	Upward aFRR bid price [€/kWh].
$\pi_{\mathrm{aFRR\ down}}$	Downward aFRR settlement price [€/kWh].
$\pi_{\mathrm{aFRR\ up}}$	Upward aFRR settlement price [€/kWh].
π_{DA}	Day-ahead market price.
$\pi_{\mathrm{FCR\ bid}}$	FCR bid price [€/MW/h].
π_{FCR}	FCR settlement price [€/MW/h].
π_{grid}	Grid tariff [€/kW].
B_s	BEB battery capacity in transaction s [kWh].
$\mathrm{C}_{\mathrm{batt}}$	Battery investment costs [€].
$\mathrm{E}_{\mathrm{dem},s}$	Energy demand of transaction s [kWh].
$\mathrm{f}_{\mathrm{act}}$	Actual grid frequency [Hz].
$\mathrm{f}_{\mathrm{nom}}$	Nominal grid frequency [Hz].
$\mathrm{P}_{\mathrm{max},s}$	Max. charging power of transaction s [kW].
$\mathrm{P}_{\mathrm{peak,max}}$	Max. peak total charging power [kW].
$\mathrm{SoC}_{\mathrm{min},s}$	Maximum SoC [%].
$\mathrm{SoC}_{\mathrm{min}}$	Minimum SoC [%].
$\mathrm{SoC}_{\mathrm{orig},t,s}$	Original SoC of transaction s at time t [%].
$\mathrm{t}_{\mathrm{arr},s}$	Starting time of transaction s.
$\mathrm{t}_{\mathrm{dep},s}$	End time of a charging transaction.

- (European Environmental Agency, 2018). Although most modes of public transport, including trains, trams and metros, are already potentially sustainable due to the electrified drive-trains, the public transport sector is still responsible for a substantial share of the total road transport emissions. In the Netherlands, the public transport sector emitted 432 kton of CO_2 in 2019, of which 90% can be attributed to buses (Kennisplatform CROW, 2020). Buses used for public transport accounted for 1.3% of the total road transport emissions in the Netherlands in 2018 (Kennisplatform CROW, 2020; CBS Statline, 2019).

To achieve the goals of the Paris Agreement and to improve the air quality in urban areas, it is important to consider low-carbon public transport solutions. The current use of fossil fuels by conventional combustion engine buses provides high potential for GHG emission reductions in the sector. Battery Electric Buses (BEBs) coupled with renewable energy sources (RES) are arguably one of the best solutions to achieve GHG emission reductions, since the emission factor of BEBs is between 19 and 92% lower compared to fossil fuel-powered buses (Lajunen and Lipman, 2016; Grijalva and López Martínez, 2019; Zhou et al., 2016).

A transition towards BEBs can be expected, since the costs of battery systems are decreasing rapidly and many governments have set targets for the adoption of zero-emission buses by bus operators. For instance, in the Netherlands, all newly-introduced buses should be zero-emission from a tank-to-wheel perspective from 2025 onward and bus fleets should be completely zero-emission by 2030 (Interprovincial Consultation et al., 2016).

Planning the introduction of BEBs in existing public transport networks requires careful consideration (Gallet et al., 2018). Large-scale adoption of BEBs by bus operators can have a significant impact on the electricity system due to the high daily driving distances of buses and their associated high energy demand for charging purposes. For instance, in the Netherlands, the annual energy demand of BEBs with a fully electrified bus sector is estimated at 500 GWh (Broos et al., 2017). BEBs charge at a high charging power rating and a large share of BEBs are often centrally charged at depots. Such a high centralized charging demand for a fully-electrified bus fleet, therefore, induces high local charging demand peaks, which could cause grid congestion problems and stress the reliability of the grid.

A transition towards BEBs also affects the daily management of bus fleets by bus operators. Fueling of conventional buses can happen in a short time span and fuel costs are not dependent on the time of the day. Charging of BEBs takes considerably longer and the costs of charging can be dependent on the moment of charging, such as under a program of Time-of-Use (ToU) tariffs for electricity (e.g., the day-ahead electricity market), and due to grid tariffs, which are related to the peak charging power at the depot.

The application of controlled charging strategies for BEBs (i.e., smart charging) could serve as an opportunity to both grid operators and bus operators. Shifting BEB charging demand to moments with low ToU tariffs or to moments with available grid capacity can result in lower charging costs for bus operators and can defer investments for costly grid reinforcements. Moreover, BEBs can contribute to maintaining the balance between supply and demand in the grid by applying BEB smart charging for the provision of balancing reserves within ancillary services markets organized by Transmission System Operators (TSOs).

The scientific literature covers a range of studies that have analyzed the potential to minimize the charging costs of BEB fleets. Some studies have proposed frameworks that minimize total costs (i.e., investment costs and operational costs) of BEBs when scheduling a BEB fleet, based on i.a. investment costs in BEBs and charging infrastructure, energy costs, battery degradation costs and labor costs, but these studies neglect ToU tariffs for electricity in the optimization process (Rogge et al., 2018; Sassi et al., 2015; Rinaldi et al., 2018; Wang et al., 2017; Zhang et al., 2021; Stumpe et al., 2021). Moradipari et al. (2020) performed a joint route assignment and charging scheduling optimization for a BEB fleet while considering ToU tariffs in the charging optimization, whereas other studies solely focused on the optimization of the charging process. Rupp et al. (2020) scheduled BEB charging using multi-objective optimization, considering day-ahead electricity prices and time-dependent CO_2-emission factors for electricity. Gao et al. (2018) and Chen et al. (2016) developed cost-minimization algorithms for BEB charging based on ToU tariffs and Raab et al. (2019) proposed an optimization framework for BEBs considering both day-ahead and intraday electricity prices. Manzolli et al. (2022) propose to use vehicle-to-grid (V2G) services to reduce charging costs for BEB charging. A framework to optimize on-route charging while considering grid constraints has been proposed by Bagherinezhad et al. (2020). Houbbadi et al. (2019) developed a system in which BEBs are charged based on ToU tariffs and battery degradation costs. The economic optimization frameworks proposed by Jahic et al. (2019) & Qin et al. (2016) only considered grid tariffs. Lymperopoulos et al. (2020) studied the technical potential and economic viability of BEBs to provide frequency restoration reserves (FRR) to the Swiss TSO.

Remarkably, only Leou and Hung (2017) and Lampropoulos et al. (2022) presented economic optimization models for BEBs that consider both of the two main cost categories: ToU tariffs and grid tariffs. Leou and Hung (2017) applied their model to a Taiwanese case study while considering a three-tariff ToU tariff system. Lampropoulos et al. (2022) presented a stochastic optimization model for bidding in the Dutch day-ahead market. These studies did not consider bidding strategies for the provision of ancillary services and neglected that BEBs could also provide V2G services. Hence, to the best knowledge of the authors, there are currently no studies in the scientific literature that compare the economic profitability, BEB charging schedules and grid impact of different BEB charging strategies with respect to electricity market participation, ancillary services provision and V2G services.

This work proposes a novel framework that can be used to model the charging process of BEBs and estimate the associated costs and grid impact for different charging strategies. The framework considers grid tariffs, day-ahead electricity market prices, V2G and two types of ancillary services that can be provided to the TSO; frequency containment reserves (FCR) and automatic FRR (aFRR). The framework can provide insight into the theoretical cost-reduction potential of different BEB charging strategies and can thus be used by bus operators as a first step to determine the economic attractiveness to move towards more-sophisticated charging strategies. The outcome of model simulations provides insight into the grid loading of bus depots for different charging strategies, which can be used by grid operators to perform grid impact analyses. The framework has been applied to a case study concerning the fleet of BEBs of one of the largest bus operators in the Netherlands.

The main contributions of this work can be outlined as follows:

- A novel framework is proposed to compare BEB charging costs and the grid impact of BEB charging for different charging strategies. The proposed framework is unique in the sense that it considers both ToU tariffs and grid tariffs in the charging model;
- A first-of-its-kind techno-economic assessment of different BEB charging strategies is presented, by applying the proposed framework to a case study using input from highly-detailed real-world BEB charging transaction data;
- Model simulations are used to determine the potential of including V2G services into the scheduling of BEB charging;
- Simulation results provide insight into the potential benefits of using BEBs for the provision of ancillary services for system balancing, i.e., FCR and aFRR provision.

Section 2 provides an overview of the research design, research scope and the formulation of the mathematical models for different charging strategies. Section 3 presents the considered case study, the data collection and the simulation outline. The results are presented in Section 4. The paper ends with discussion in Section 5 and conclusions in Section 6.

2. Research design and scope

2.1. Scope and system overview

This work proposes a framework that can be used to determine the charging costs for different charging strategies for BEBs at bus depots. The charging costs for every charging strategy can be compared with the required investments and operational costs for every charging strategy to determine the optimal charging strategy for a bus operator. Since these costs are very case-specific, they are out of the scope of this work.

Models to determine the charging schedules of BEBs at bus depots for different charging strategies are presented in this work. These models can be applied to bus timetables or to historical BEB charging transaction data. The latter can only be used in case the charging process of the BEBs (recorded in the historical charging data) has not been optimized to assure that the considered charging demand of each charging transaction in the model simulations represents the maximum possible charging demand in the timeframe between the arrival and departure time of the specific BEB.

A depot hosts a set of chargers which are used by BEBs that are not in service to recharge their battery for upcoming trips. Opportunity charging of buses during their service is therefore out of the scope of this research. A depot is assumed to be connected to the electricity grid through a grid connection that is not used by other grid loads.

The power of the available chargers can be controlled by the bus operator directly or via an aggregator. This provides opportunities to adjust the charging schedules of BEBs in order to minimize their charging costs. Charging costs can be reduced by (i) minimizing peak demand for electricity, which impacts the grid fees, (ii) charging at moments with beneficial ToU tariffs, (iii) receiving financial compensation for the provision of ancillary services to the TSO, and (iv) minimizing battery degradation costs.

This study considers four charging strategies for the scheduling of BEBs, which are summarized as follows:

1. Charging-on-arrival: In this reference charging strategy, all BEBs start charging at the time of arrival at the nominal capacity of the charger until the charging demand is satisfied.
2. Peak-shaving: BEBs optimize their charging schedules to limit the peak demand from the grid by spreading the charging demand of BEBs over time. Lower peak demands result in a reduction of grid tariffs, which are in many countries based on the monthly and annual demand peaks of a grid connection (European Union Agency for the Cooperation of Energy Regulators, 2021).
3. Day-ahead market trade excluding V2G functions: The day-ahead markets provides hourly electricity prices. As the market prices for the next day can be forecasted with a relatively high degree of accuracy (Lago et al., 2018), the charging of BEBs may be optimized by shifting consumption to the lower-priced hours. This charging strategy also considers grid tariffs, since the benefits of charging at moments with low electricity prices can be offset by higher grid tariffs induced by new demand peaks.
4. Day-ahead market trade including V2G functions: Extra benefits of day-ahead market trading can be obtained by feeding electricity back to the grid using V2G technology at moments with relatively high day-ahead prices. This charging strategy is an extension of the previous charging strategy, by also considering V2G functions for BEB charging. Grid tariffs are also considered in this charging strategy.

Two additional charging strategies for participating in ancillary services markets are considered, i.e. the provision of FCR and aFRR for system balancing. These strategies require charging schedules from BEBs using one of the four aforementioned charging strategies as an input. These two strategies for participating in the ancillary service markets are outlined as follows:

1. Provision of FCR: TSOs contract FCR, which are automatically activated based on frequency deviations in the electricity system to restore the system frequency when supply–demand imbalances occur. Battery systems, such as BEBs, are regarded as an attractive technology for the provision of FCR due to their short activation time (Münderlein et al., 2019; Zhang et al., 2018). This strategy evaluates the possibility and attractiveness of BEBs charging processes to participate in FCR auctions.
2. Provision of aFRR: After the initial activation of FCR, TSOs activate aFRR, based on Area Control Error (ACE) calculations to restore the balance between supply and demand of electricity. This strategy studies the potential of BEB batteries to participate in the aFRR market.

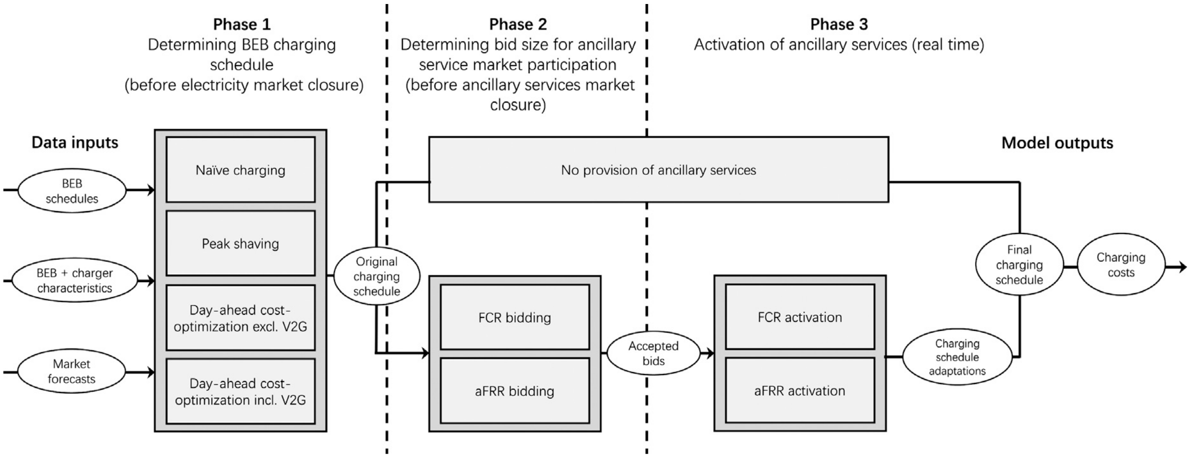

Fig. 1. Schematic overview of the relationship between the different considered charging strategies.

More information on these ancillary services markets is provided in Appendix.

Fig. 1 provides a schematic overview of the temporal sequence of the different considered BEB charging strategies, including the required data inputs, as well as the data flows between the different charging strategies. The initial charging strategies of BEBs are determined in Phase 1, using BEB driving schedules, charging infrastructure characteristics and electricity market forecasts. If the provision of FCR or aFRR is considered, bids to the corresponding auction are made in Phase 2, building upon the initial charging schedules determined in Phase 1. The bids made available in Phase 2 might be activated for the provision of ancillary services in real-time, which results in adaptations of the initial charging schedules.

This study aims to create insight into the theoretical potential of participating in different electricity and ancillary services markets by controlling the charging processes of BEBs. A number of assumptions have been made, underlining the developed mathematical models, which are listed herein for providing clarity to the reader:

- In all considered charging models, including the ancillary service market models, the charging demand of a charging transaction cannot be compromised and should be satisfied at the departure time, to assure that the application of a specific charging strategy does not affect the daily operation of BEBs;
- The day-ahead and peak-shaving strategies are implemented as deterministic models, assuming perfect foresight in the day-ahead electricity prices and in the different characteristics of the charging transactions (arrival time, departure time, charging demand and the maximum charging power);
- No perfect foresight in market prices is assumed in the ancillary service market models;
- No other loads than the charging of BEBs is considered when determining the grid tariffs;
- V2G functions are assumed to be available for the provision of ancillary services, to get insight into the maximum potential of BEBs to provide ancillary services;
- Investments, operational costs and maintenance costs associated with each charging strategy fall outside the scope of this research;
- Constant current constant voltage (CC-CV) charging characteristics of lithium-ion batteries (Wang et al., 2021) are not considered, as such detailed characteristics would add significant computational burden in the simulation model with negligible effect on the modeled charging profiles and in the final cost calculations.

2.2. Charging model formulation

The mathematical formulations for the four proposed strategies for the scheduling of BEBs in Phase 1 are outlined in this section.

2.2.1. Charging-on-arrival

As indicated, this strategy serves as the reference case, and is used further for benchmarking purposes. It simulates an uncontrolled charging method, meaning that once a BEB arrives at the depot, the charging process starts immediately and continues until the charging demand of the BEB is satisfied.

This model uses a heuristic approach. For each charging transaction s within the set $\mathcal{S}$ (indexed by $s = 1, 2, \ldots, S$), the BEB charges at the maximum possible charging power of the charging transaction ($\mathrm{P}_{\max,s}$) directly after its time of arrival at the depot

($t_{arr,s}$), until its charging demand ($E_{dem,s}$) is satisfied. The charging power of an individual charging transaction ($P_{ch,t,s}$) at the BEB battery at time step t is modeled as follows:

$$P_{ch,t,s} = \begin{cases} P_{max,s}, & \text{if } E_{dem,s} \geq P_{max,s}\Delta t, \forall t \in \{t_{arr,s}\}, \\ \frac{E_{dem,s}}{\Delta t}, & \text{if } E_{dem,s} < P_{max,s}\Delta t, \forall t \in \{t_{arr,s}\}, \\ P_{max,s}, & \text{if } E_{dem,s} \geq \sum_{\tau=t_{arr,s}}^{t-\Delta t}(P_{ch,\tau,s}\Delta t) + P_{max,s}\Delta t, \forall t \in \{t_{arr,s}+\Delta t, \dots, t_{dep,s}\}, \\ \frac{E_{dem,s}}{\Delta t} - \sum_{\tau=t_{arr,s}}^{t-\Delta t} P_{ch,\tau,s}, & \text{if } E_{dem,s} < \sum_{\tau=t_{arr,s}}^{t-\Delta t}(P_{ch,\tau,s}\Delta t) + P_{max,s}\Delta t, \forall t \in \{t_{arr,s}+\Delta t, \dots, t_{dep,s}\}, \end{cases} \forall s, \tag{1}$$

where Δt is the duration of one time step, τ is one of the time steps before time step t and $t_{dep,s}$ is the departure time of transaction s.

2.2.2. Peak-shaving

The peak-shaving charging strategy is formulated as the following optimization problem:

$$\underset{P_{ch}, P_{peak}, P_{ch,tot}}{\text{minimize}} \quad P_{peak}\pi_{grid} \tag{2a}$$

$$\text{subject to} \quad 0 \leq P_{ch,t,s} \leq P_{max,s} \;\; \forall t \in \{t_{arr,s}, \dots, t_{dep,s}\}, s, \tag{2b}$$

$$\sum_{t=t_{arr}}^{t_{dep,s}} P_{ch,t,s}\Delta t = E_{dem,s} \;\; \forall s, \tag{2c}$$

$$P_{ch,tot,t} = \sum_{s=1}^{S} \frac{1}{\eta_{ch}} P_{ch,t,s} \;\; \forall t, \tag{2d}$$

$$P_{peak} = \max\{P_{ch,tot,t=1}, P_{ch,tot,t=2}, \dots, P_{ch,tot,t=T}\}. \tag{2e}$$

The objective of the function in Eq. (2a) is to minimize grid tariffs, where P_{peak} represents the peak charging power of all BEBs during the assessment timeframe $\mathcal{T}$ (indexed by $t = 1, 2, \dots, T$) in kW and π_{grid} represents the grid tariff in €/kW. Since electricity tariffs are assumed to be time-independent for this charging strategy, electricity costs are not considered in the objective function. The charging power of BEBs is constrained by the maximum charging power in transaction s according to Eq. (2b). Constraint (2c) assures that the charging demand of every charging transaction is met before unplugging. The total combined charging power of all charging transactions at each time step ($P_{ch,tot}$) is defined in constraint (2d), where η_{ch} represents the charging efficiency. P_{peak} is equal to the maximum value of $P_{ch,tot}$, as expressed in constraint (2e).

2.2.3. Day-ahead market trading excluding V2G functions

The optimization problem of the charging strategy which also considers cost-minimization in the day-ahead market is formulated as follows:

$$\underset{P_{ch}, P_{peak}, P_{ch,tot}}{\text{minimize}} \quad \sum_{t=1}^{T} (P_{ch,tot,t}\pi_{DA,t})\Delta t + P_{peak}\pi_{grid} \quad \text{subject to} \quad \text{(2b)–(2e)}. \tag{3}$$

The objective function minimizes the sum of the electricity costs (first part of Eq. (3)) and grid tariffs (second part of Eq. (3)), where $\pi_{DA,t}$ represents the time-dependent day-ahead market price. If there is any discrepancy between the assessment period for grid fees (e.g., if these are calculated on a monthly or annual basis), a correction factor with the ratio between model simulation period and the assessment period should be applied to the grid tariffs. All constraints are identical to the peak-shaving model described in Section 2.2.2.

2.2.4. Day-ahead market trading including V2G functions

The day-ahead market trading charging strategy including V2G functions is formulated as the following optimization problem:

$$\underset{\substack{P_{ch}, P_{disch}, P_{peak}, P_{ch,tot}, \\ P_{disch,tot}, C_{deg}, SoC}}{\text{minimize}} \quad \sum_{t=1}^{T} ((P_{ch,tot,t} - P_{disch,tot,t})\pi_{DA,t})\Delta t + P_{peak}\pi_{grid} + C_{deg} \tag{4a}$$

$$\text{subject to} \quad C_{deg} = \sum_{s=1}^{S}\sum_{t=t_{arr}}^{t_{dep,s}} C_{batt,s}\Phi(SoC_{t,s} - SoC_{t-\Delta t,s}), \tag{4b}$$

$$SoC_{t,s} = SoC_{t_{arr,s},s} + \sum_{\tau=t_{arr,s}}^{t-\Delta t} \frac{(P_{ch,\tau,s} - P_{disch,\tau,s}\Delta t)}{B_s} \;\; \forall t \in \{t_{arr,s}, \dots, t_{dep,s}\}, s, \tag{4c}$$

$$SoC_{min} \leq SoC_{t,s} \leq SoC_{max} \;\; \forall t \in \{t_{arr,s}, \dots, t_{dep,s}\}, s, \tag{4d}$$

$$0 \leq P_{disch,t,s} \leq P_{max,s} \;\; \forall t \in \{t_{arr,s}, \dots, t_{dep,s}\}, s, \tag{4e}$$

$$\sum_{t=t_{\mathrm{arr}}}^{t_{\mathrm{dep},s}} (P_{\mathrm{ch},t,s} - P_{\mathrm{disch},t,s})\Delta t = E_{\mathrm{dem},s} \ \forall s, \tag{4f}$$

$$P_{\mathrm{disch,tot},t} = \sum_{s=1}^{S} \eta_{\mathrm{disch}} P_{\mathrm{disch},t,s} \ \forall t, \tag{4g}$$

$$P_{\mathrm{peak}} = \max\{|P_{\mathrm{ch,tot},t=1} - P_{\mathrm{disch,tot},t=1}|, \ldots, |P_{\mathrm{ch,tot},t=T} - P_{\mathrm{disch,tot},t=T}|\}, \tag{4h}$$

$$(2d) \ \& \ (2e). \tag{4i}$$

Since V2G functions are considered in this charging strategy, the discharging of BEBs is also included through the variables P_{disch} and $P_{\mathrm{disch,tot}}$, which represent the discharging power rate for one BEB and the total discharging power for all BEBs respectively. The objective function in this optimization problem (4a) is different in two aspects compared to the objective function from the sub-problem described in Section 2.2.3. First, the financial benefits of discharging BEBs are considered in the objective function. Second, battery degradation costs (C_{deg}) are considered in the objective function, since a high number of BEB charging/discharging cycles can induce cyclic aging of the BEB battery (Swierczynski et al., 2015; Stroe et al., 2017), shortening the battery lifetime. By including cyclic battery degradation costs in the objective function, it is ensured that the extra financial benefits of an extra charging/discharging cycle exceed the extra battery degradation costs of this cycle.

Battery degradation costs are formulated in constraint (4b), which are dependent on the battery investment costs C_{batt} and a dimensionless degradation function Φ, which is outlined in Brinkel et al. (2020) and is a function of the change in battery state of charge (SoC) between two time steps. $SoC_{t,s}$ represents the SoC at the beginning of a time step for charging transaction s and is defined in constraint (4c). It depends on the overall charging energy of the specific charging transaction between $t_{\mathrm{arr},s}$ and t and the battery capacity of the BEB (B_s) in the specific charging transaction. The SoC is constrained by the minimum and maximum SoC ($SoC_{\min}$/$SoC_{\max}$) in constraint (4d). The discharging power of the BEB is bounded by constraint (4e). Constraint (4f) assures that the net charging energy at the end of a charging transaction equals the charging demand. $P_{\mathrm{disch,tot}}$ is defined in (4g). In this constraint, η_{disch} represents the discharging efficiency. P_{peak} equals the highest absolute value of the difference between $P_{\mathrm{ch,tot}}$&$P_{\mathrm{disch,tot}}$. Lastly, this model also considers constraints (2d) & (2e).

2.3. Ancillary service provision problem formulation

After the scheduling of BEBs using one of the aforementioned charging strategies (Phase 1 in Fig. 1), the bus fleet operator can participate in one of the specified ancillary services markets organized by the TSO (Phase 2 & 3 in Fig. 1). Participation in one of these balancing markets comprises different steps that need to be modeled separately:

1. The bus fleet operator or the aggregator needs to determine the bid size and bid price to be submitted to the market;
2. The bid will be accepted or rejected based on the bid price, which is determined based on the overall bid ladder and system imbalance;
3. Charging of BEBs is adjusted based on the grid frequency deviation or on the activation signal sent by the TSO.

This section addresses models for participation in the aFRR and FCR markets organized by the TSO. To obtain insight in the full potential of BEBs to provide ancillary services, these models assume that V2G functions are available. In practice, a bus fleet operator can also decide to limit V2G functions for the use of ancillary service provision, reducing its potential to provide these balancing reserves to the ancillary service markets.

2.3.1. Participation in the FCR market

TSOs organize auctions to contract FCR capacity for a predefined period. If the bid of a market participant is accepted, this market participant must assure that its assets can offer the bidded capacity as both upward and downward FCR reserves[2] during the whole auction period.

Bid size The maximum potential bid size for every time step of the transaction is determined based on the maximum symmetrical power that can be provided at a full activation deviation moment (Δf_{full}; i.e., frequency deviation where the bidded capacity is expected to be fully activated, as set by TSOs in the FCR product requirements (ENTSO-E, 2022)). Since BEBs must be able to provide this power symmetrically, the potential to provide upward and downward FCR reserves must be determined separately.

The upward and downward potential to provide FCR for an individual charging transaction ($P_{\mathrm{FCR\ up\ max},t,s}$/$P_{\mathrm{FCR\ down\ max},t,s}$) can be constrained by two factors. First, it is constrained by the charging power of the charger or the bus; the total charging power of a charging transaction when considering both the original charging/discharging schedule and the alterations to these schedules for the provision of FCR should remain between $-P_{\max,s}$ and $P_{\max,s}$. Second, BEBs can only provide FCR if the $SoC_{t,s}$ remains between $SoC_{\min}$ and $SoC_{\max}$. Based on these conditions, $P_{\mathrm{FCR\ up\ max},t,s}$&$P_{\mathrm{FCR\ down\ max},t,s}$ can be determined for each charging transaction at each time step as follows:

[2] Upward FCR and aFRR reserves correspond to an increase in generation and/or a decrease in consumption and downward FCR and aFRR reserves correspond to a reduction in generation and/or an increase in consumption compared to the reference schedule (ENTSO-E, 2019). In the case of the provision of FCR/aFRR through BEB charging, upward FCR and aFRR reserves correspond to a decrease in charging power or an increase in V2G injection volumes, and downward FCR and aFRR reserves correspond to an increase in charging power or a decrease in V2G injection volumes.

$$P_{\text{FCR up max},t,s} = \begin{cases} \frac{(\text{SoC}_{t,s} - \text{SoC}_{\min})\text{B}_s}{\Delta t} + P_{\text{ch},t,s} - P_{\text{disch},t,s} & \text{if } \frac{(\text{SoC}_{t,s} - \text{SoC}_{\min})\text{B}_s}{\Delta t} \leq P_{\max,s} \\ P_{\max,s} + P_{\text{ch},t,s} - P_{\text{disch},t,s} & \text{if } \frac{(\text{SoC}_{t,s} - \text{SoC}_{\min})\text{B}_s}{\Delta t} > P_{\max,s} \end{cases} \forall t \in \{t_{\text{arr},s}, \dots, t_{\text{dep},s}\}, s, \tag{5}$$

$$P_{\text{FCR down max},t,s} = \begin{cases} \frac{(\text{SoC}_{\max} - \text{SoC}_{t,s})\text{B}_s}{\Delta t} - (P_{\text{ch},t,s} - P_{\text{disch},t,s}) & \text{if } \frac{(\text{SoC}_{\max} - \text{SoC}_{t,s})\text{B}_s}{\Delta t} \leq P_{\max,s} \\ P_{\max,s} - (P_{\text{ch},t,s} - P_{\text{disch},t,s}) & \text{if } \frac{(\text{SoC}_{\max} - \text{SoC}_{t,s})\text{B}_s}{\Delta t} > P_{\max,s} \end{cases} \forall t \in \{t_{\text{arr},s}, \dots, t_{\text{dep},s}\}, s. \tag{6}$$

Subsequently, $P_{\text{FCR up max},t,s}$&$P_{\text{FCR down max},t,s}$ are summed over all charging transactions to obtain the total upward and downward FCR power that a fleet of BEBs can provide at time t ($P_{\text{FCR up fleet max},t}$/$P_{\text{FCR down fleet max},t}$):

$$P_{\text{FCR up fleet max},t} = \eta_{\text{disch}} \sum_{s=1}^{S_t} P_{\text{FCR up max},t,s} \ \forall t, \tag{7}$$

$$P_{\text{FCR down fleet max},t} = \frac{1}{\eta_{\text{ch}}} \sum_{s=1}^{S_t} P_{\text{FCR down max},t,s} \ \forall t, \tag{8}$$

where S_t is the set of charging transactions connected to a charger at time t.

An accepted bid for the provision of FCR must be able to offer the accepted bid size as both upward and downward reserves during the whole auction period. The maximum bid size at time t ($P_{\text{FCR fleet max},t}$) is therefore defined as follows:

$$P_{\text{FCR fleet max},t} = \min\{P_{\text{FCR up fleet max},t}, P_{\text{FCR down fleet max},t}\} \forall t. \tag{9}$$

The maximum bid size during auction i is equal to the minimum value of $P_{\text{FCR fleet max},t}$ between the first and the last time step of this auction period (t_{i1} and T_i respectively):

$$P_{\text{FCR fleet max},i} = \min\{P_{\text{FCR fleet max},t_{i1}}, P_{\text{FCR fleet max},t_{i1}+\Delta t}, \cdots, P_{\text{FCR fleet max},T_i}\} \forall i \in I, \tag{10}$$

where $\mathcal{I}$ is the set of FCR auctions in the assessment timeframe (indexed by $i = 1, 2 \dots, I$).

As a side effect, grid tariffs can increase when BEBs provide ancillary services, since the activation of BEB charging/discharging for the provision of FCR can induce high charging or discharging peaks. For this reason, bus operators can decide to restrict the FCR bid size to assure that the peak charging or discharging power in case of full FCR activation does not violate a predetermined value $P_{\text{peak,max}}$. The maximum FCR power that can be provided without risking that $P_{\text{peak,max}}$ is exceeded (defined as $P_{\text{FCR grid max}}$) at time t is based on the difference between $P_{\text{peak,max}}$ and the absolute total charging power at this time step:

$$P_{\text{FCR grid max},t} = P_{\text{peak,max}} - |P_{\text{ch,tot},t} - P_{\text{disch,tot},t}| \ \forall t. \tag{11}$$

The total amount of FCR power that can be provided during one auction period without exceeding $P_{\text{peak,max}}$ is equal to the lowest value of $P_{\text{FCR grid max},t}$ in the auction period:

$$P_{\text{FCR grid max},i} = \min\{P_{\text{FCR grid max},t_{i1}}, P_{\text{FCR grid max},t_{i1}+\Delta t}, \cdots, P_{\text{FCR grid max},T_i}\} \ \forall i. \tag{12}$$

The actual FCR bid size during auction period i ($P_{\text{FCR bid},i}$) is the minimum of $P_{\text{FCR fleet max},i}$ and $P_{\text{FCR grid max},i}$:

$$P_{\text{FCR bid},i} = \min\{P_{\text{FCR fleet max},i}, P_{\text{FCR grid max},i}\} \ \forall i. \tag{13}$$

Bid acceptance Acceptance of a submitted FCR bid depends on the associated FCR bid price $\pi_{\text{FCR bid},i}$. An FCR bid is only accepted if $\pi_{\text{FCR bidded},i}$ is below the FCR settlement price $\pi_{\text{FCR},i}$. Acceptance of bid size during auction i ($P_{\text{FCR accepted bid},i}$) is formulated as follows:

$$P_{\text{FCR accepted bid},i} = \begin{cases} P_{\text{FCR bid},i} & \text{if } \pi_{\text{FCR bid},i} \leq \pi_{\text{FCR},i} \\ 0 & \text{if } \pi_{\text{FCR bid},i} > \pi_{\text{FCR},i} \end{cases} \forall i. \tag{14}$$

FCR activation The accepted FCR bid size will only be fully activated if the deviation from the nominal frequency (f_{nom}) exceeds Δf_{full}. If the deviation from the nominal frequency is below the minimum deviation for FCR activation ($\Delta f_{\min}$), the bid will not be activated. Any deviation between $\Delta f_{\min}$&Δf_{full} results in partial activation of the accepted FCR bid size:

$$P_{\text{FCR activated},t} = \begin{cases} P_{\text{FCR accepted bid},i} & \text{if } (f_{\text{act},t} - f_{\text{nom}}) < -\Delta f_{\text{full}} \\ P_{\text{FCR accepted bid},i} \frac{f_{\text{nom},t} - f_{\text{act}}}{\Delta f_{\text{full}}} & \text{if } -\Delta f_{\text{full}} \leq (f_{\text{act},t} - f_{\text{nom}}) \leq -\Delta f_{\min} \\ 0 & \text{if } -\Delta f_{\min} < (f_{\text{act},t} - f_{\text{nom}}) < \Delta f_{\min} \\ -P_{\text{FCR accepted bid},i} \frac{f_{\text{nom},t} - f_{\text{act}}}{\Delta f_{\text{full}}} & \text{if } \Delta f_{\min} \leq (f_{\text{act},t} - f_{\text{nom}}) \leq \Delta f_{\text{full}} \\ -P_{\text{FCR accepted bid},i} & \text{if } (f_{\text{act},t} - f_{\text{nom}}) > \Delta f_{\text{full}} \end{cases} \forall i, t \in \{t_{i1}, \dots, T_i\}, \tag{15}$$

where $P_{\text{FCR activated},t}$ represents the activated FCR power at time t and $f_{\text{act},t}$ represents for the actual frequency at time t. These equations are based on the work of Steber et al. (2017).

2.3.2 Participation in the aFRR market

The threshold for participating in the aFRR market is lower than when participating in the FCR market, since both markets differ from each other in three aspects. First, it is not necessary to be contracted for a full auction period when participating using bids for non-contracted aFRR (Lampropoulos et al., 2018). A market participant can make separate bids for each Imbalance Settlement Period (ISP) and can also decide to not participate in specific ISPs. Second, aFRR is an asymmetrical product, meaning that a market participant can make separate bids for upward and downward aFRR for every ISP. Third, the minimum response time is lower when providing aFRR.

Bid size Similar to the methods used to determine the FCR bid size, the maximum downward aFRR power that can be offered to the TSO ($P_{\text{aFRR down max},t,s}$) is constrained by the upper limit of the SoC and the maximum charging power of the charger or bus:

$$P_{\text{aFRR down max},t,s} = \begin{cases} \frac{(\text{SoC}_{\max} - \text{SoC}_{t,s})B_s}{\Delta t} - (P_{\text{ch},t,s} - P_{\text{disch},t,s}) & \text{if } \frac{(\text{SoC}_{\max} - \text{SoC}_{t,s})B_s}{\Delta t} \le P_{\max,s}, \\ P_{\max,s} - (P_{\text{ch},t,s} - P_{\text{disch},t,s}) & \text{if } \frac{(\text{SoC}_{\max} - \text{SoC}_{t,s})B_s}{\Delta t} > P_{\max,s}, \end{cases} \forall t \in \{t_{\text{arr},s}, \dots, t_{\text{dep}}\}, s, \tag{16}$$

When determining the maximum upward aFRR power ($P_{\text{aFRR up max},t,s}$) that can be provided by a charging transaction, it is assured that the SoC never gets below the SoC of the original charging schedule $\text{SoC}_{\text{orig},t,s}$. In this way, the charging volume during a transaction is at least as high in the original charging schedule, assuring that a BEB's charging demand is satisfied. Effectively, this means that a charging transaction can only provide upward aFRR power if it previously has provided downward aFRR power. This is outlined using the following equations:

$$P_{\text{aFRR up max},t,s} = \begin{cases} \frac{(\text{SoC}_{t,s} - \text{SoC}_{\text{org},t,s})B_s}{\Delta t} + P_{\text{ch},t,s} - P_{\text{disch},t,s} & \text{if } \frac{(\text{SoC}_{t,s} - \text{SoC}_{\text{org},t,s})B_s}{\Delta t} \le P_{\max,s}, \\ P_{\max,s} + P_{\text{ch},t,s} - P_{\text{disch},t,s} & \text{if } \frac{(\text{SoC}_{t,s} - \text{SoC}_{\text{org},t,s})B_s}{\Delta t} > P_{\max,s}, \end{cases} \forall t \in \{t_{\text{arr},s}, \dots, t_{\text{dep}}\}, s. \tag{17}$$

In both Eq. (16) and (17), $\text{SoC}_{t,s}$ is updated based on the aFRR activation in previous time steps:

$$\text{SoC}_{t,s} = \text{SoC}_{\text{org},t,s} + \sum_{\tau = t_{\text{arr},s}}^{t-\Delta t} \frac{(P_{\text{aFRR down activated},\tau,s} - P_{\text{aFRR up activated},\tau,s})\Delta t}{B_s} \forall t \in \{t_{\text{arr},s}, \dots, t_{\text{dep}}\}, s. \tag{18}$$

where $P_{\text{aFRR up activated},t,s}$&$P_{\text{aFRR down activated},t,s}$ are the activated upward and downward aFRR power of transaction s at time t, respectively.

Subsequently, the maximum aggregated bid size for upward and downward aFRR for the fleet of BEBs ($P_{\text{aFRR up fleet max},t}$/$P_{\text{aFRR down fleet max},t}$) is determined by summing $P_{\text{aFRR up max},t,s}$ and $P_{\text{aFRR down max},t,s}$ over the set of charging transactions:

$$P_{\text{aFRR up fleet max},t} = \eta_{\text{disch}} \sum_{s=1}^{S_t} P_{\text{aFRR up max},t,s} \ \forall t, \tag{19}$$

$$P_{\text{aFRR down fleet max},t} = \frac{1}{\eta_{\text{ch}}} \sum_{s=1}^{S_t} P_{\text{aFRR down max},t,s} \ \forall t. \tag{20}$$

To avoid high grid tariffs induced by high BEB charging or discharging peaks caused by aFRR activation, bus operators can also limit the aFRR bid size to avoid that the total charging and discharging peak exceeds the predetermined value $P_{\text{peak,max}}$. The upward and downward aFRR power ($P_{\text{aFRR grid up max}}$/$P_{\text{aFRR grid down max}}$) that can be provided without risking exceedance of $P_{\text{peak,max}}$ is determined as follows:

$$P_{\text{aFRR grid up max},t} = P_{\text{peak,max}} - (P_{\text{disch,tot},t} - P_{\text{ch,tot},t}) \ \forall t, \tag{21}$$

$$P_{\text{aFRR grid down max},t} = P_{\text{peak,max}} - (P_{\text{ch,tot},t} - P_{\text{disch,tot},t}) \ \forall t. \tag{22}$$

The upward and downward aFRR bid sizes at time t ($P_{\text{aFRR bid up}}$/$P_{\text{aFRR bid down}}$) are subsequently defined using the following equations:

$$P_{\text{aFRR bid up},t} = \min\{P_{\text{aFRR fleet up max},t}, P_{\text{aFRR grid up max},t}\} \ \forall t, \tag{23}$$

$$P_{\text{aFRR bid down},t} = \min\{P_{\text{aFRR fleet down max},t}, P_{\text{aFRR grid down max},t}\} \ \forall t. \tag{24}$$

aFRR bid acceptance and activation An upward aFRR bid is accepted and activated if the imbalance or activation price ($\pi_{\text{aFRR up},t}$) is higher than or equal to the bid price $\pi_{\text{aFRR up bid},t}$. Conversely, a downward aFRR bid is accepted and activated if the bid price $\pi_{\text{aFRR down bid},t}$ is higher than or equal to the imbalance price $\pi_{\text{aFRR down},t}$:

$$P_{\text{aFRR up activated},t} = \begin{cases} P_{\text{aFRR up bid},t} & \text{if } \pi_{\text{aFRR up bid},t} \ge \pi_{\text{aFRR up},t} \\ 0 & \text{if } \pi_{\text{aFRR up bid},t} < \pi_{\text{aFRR up},t} \end{cases} \forall t, \tag{25}$$

$$P_{\text{aFRR down activated},t} = \begin{cases} P_{\text{aFRR bid down},t} & \text{if } \pi_{\text{aFRR down bid},t} \le \pi_{\text{aFRR down},t} \\ 0 & \text{if } \pi_{\text{aFRR down bid},t} > \pi_{\text{aFRR down},t} \end{cases} \forall t, \tag{26}$$

where $P_{\text{aFRR up activated},t}$ & $P_{\text{aFRR down activated},t}$ represent the activated upward and downward aFRR power for the fleet of BEBs.

Table 1
Overview of the different considered combinations of BEB charging strategies and participation strategies in the ancillary services markets in this research.

	BEB charging strategy	Ancillary services participation
1. Charging-on-arrival	Charging-on-arrival	–
2. Peak-shaving	Peak-shaving	–
3. DAM trading without V2G	Day-ahead cost-optimization excl. V2G	–
4. DAM trading with V2G	Day-ahead cost-optimization incl. V2G	–
5. DAM trading (without V2G) + FCR[a]	Day-ahead cost-optimization excl. V2G	FCR
6. DAM trading (without V2G) + aFRR[a]	Day-ahead cost-optimization excl. V2G	aFRR

[a]Model simulations are performed for different bid prices for participation in the aFRR and FCR market and for different maximum peak grid loads ($P_{peak,max}$), as outlined in Section 4.1.1.

2.4 Evaluation

The attractiveness of the proposed charging strategies can be determined by comparing the overall charging costs to the bus operator (C) for different charging strategies:

$$C = \sum_{t=1}^{T}((P_{ch,tot,t} - P_{disch,tot,t})\pi_{DA,t})\Delta t + P_{peak}\pi_{grid} - \sum_{i=1}^{I}(P_{FCR\ accept,i}\pi_{FCR,i}) - \sum_{t=1}^{T}(P_{aFRR\ up\ activated,t}\pi_{aFRR\ up,t})\Delta t + \sum_{t=1}^{T}(P_{aFRR\ down\ activated,t}\pi_{aFRR\ down,t})\Delta t + C_{deg} \quad (27)$$

The first two terms of Eq. (27) represent the BEB charging costs and the grid fees, identical to Eq. (4a). As discussed in Section 2.2.3, a correction factor might be applied to the grid fees. The third term represents the revenues for participating in the FCR market. In Europe, the compensation to a market participant is solely based on the FCR capacity that is offered to the TSO and is independent on the activated FCR volumes. This market uses the marginal pricing principle, which means that the compensation for a market participant is equal to the FCR settlement price (ENTSO-E, 2021). The fourth and fifth terms of Eq. (27) represent the financial settlement for the provision of aFRR. In contrast to the FCR market, the aFRR financial settlement is based on the activated aFRR volumes of the market participant. The market also uses the marginal pricing principle (ENTSO-E, 2019). The market participant receives the aFRR price for the provision of upward aFRR reserves and pays the aFRR price for the provided downward aFRR reserves.[3] The last term in the equation represents the battery degradation costs.

3 Data inputs & simulation outline

3.1 Case study specifications

Qbuzz is one of the largest bus operators in the Netherlands, operating in three main regions. It operates approximately 700 buses and had a market share in the Netherlands of 14% in 2017 (Broos et al., 2017). The size of the total BEB fleet of Qbuzz grew from 180 BEBs at the beginning of 2020 to 259 BEBs by the end of 2020. Three of their charging depots will serve as a case study in this research. The largest charging depot (referred to as 'Location A') hosted 101 BEBs at the beginning of 2020. The second depot ('Location B') and third depot ('Location C') were considerably smaller, serving 39 BEBs and 13 BEBs respectively at this time. Where the bus lines at Location B and C mostly serve urban areas, a relatively large share of the bus lines at Location A serve rural areas, resulting in a longer average trip distance and a longer average charging demand per charging transaction at this location. The arrival times of BEBs show similar trends between the three considered locations, with peaks in the arrival of BEBs at the end of the morning (10:00-12:00) and in the early evening (18:00-19:00).

3.2 Simulation outline

A total of six combinations of BEB charging strategies and strategies for participating in the ancillary services market are considered in the model simulations. Given the large number of possible combinations of BEB charging strategies and ancillary services participation strategies, only one BEB charging strategy is considered for each ancillary services participation strategy in the model simulations. All considered combinations are outlined in Table 1.

The first four combinations in Table 1 consider each of the considered BEB charging strategies outlined in Section 2.1 without participation in an ancillary services market. The last two combinations consider day-ahead charging without V2G in combination with each of the two considered ancillary services markets introduced in Section 2.1. All model simulations were performed using historical BEB charging transaction data as inputs. The observed charging demand, maximum charging power and arrival and departure time of charging transaction s in the historical dataset are used as the values for $E_{dem,s}$, $P_{max,s}$, $t_{arr,s}$ and $t_{dep,s}$ in the model

[3] Note that the downward aFRR price is generally lower than the day-ahead market price, making it financially attractive to provide downward aFRR reserves.

Table 2
Overview of considered data inputs for the different model simulations.

Symbol	Description	Value
Δt	Time step duration	15 min
Δt_{FCR}	Time step duration for FCR modeling	5 min
η_{ch}	Charging efficiency	$\sqrt{0.87}$ (Schram et al., 2020)
η_{disch}	Discharging efficiency	$\sqrt{0.87}$ (Schram et al., 2020)
π_{grid}	Grid fees	2.4147 €/kW/month (Stedin DSO, 2019)
$\pi_{aFRR\ down\ bid}$	Considered bid pricesfor down aFRR	Different values between−1 and −100 €/MWh[a]
$\pi_{aFRR\ up\ bid}$	Considered bid pricesfor upward aFRR	Different values between1 and 100 €/MWh[a]
$\pi_{FCR\ bidded}$	Considered FCR bid prices	Different values between0 and 12 €/MW/h
$P_{peak,max}$	Considered maximum peak powerfor ancillary service market participation	Different values per considered location,as outlined in Section 4.1.1.
Φ	Battery degradation function & parameters	Values from Brinkel et al. (2020)
SoC_{min}	Minimum SoC	20%
SoC_{max}	Maximum SoC	100%

[a]Market participants usually base their aFRR bids on the day-ahead market price (Vas-Corrales et al., 2021). For this reason, the reported aFRR bid prices represent the difference with the day-ahead market price at a specific moment.

simulations for all considered charging strategies. Although day-ahead prices are not considered in the optimization of the 'charging-on-arrival' and 'peak-shaving' charging strategies, the charging costs of these strategies are evaluated using day-ahead prices to allow for a fair comparison between the different charging strategies. The model simulations were conducted in Python (Python Software Foundation, 2022) with the Gurobi optimizer (Gurobi, 2022), using a high computing cluster with 250 GB RAM per node.

3.3 Data collection

3.3.1 BEB charging transaction data

This study considered three weeks of charging data between 20 February 2020 and 11 March 2020 for the selected depots. The BEB charging data contains for each charging transaction the arrival and departure time of the BEB at the depot, the energy consumption during the charging transaction, the maximum charging power of the charger and the SoC at the arrival and departure time. All BEBs in the considered case study followed a 'charging-on-arrival' strategy. The provided dataset contains 1213 transactions from 101 BEBs for Location A, 714 transactions from 39 unique BEBs for Location B and 163 transactions from 13 unique BEBs for Location C.

3.3.2 Day-ahead electricity market price data and ancillary services market price data

Day-ahead market prices and aFRR prices for up- and downward regulation from 20 February 2020 to 11 March 2020 were retrieved from the ENTSO-E Transparency platform (ENTSO-E, 2022). The FCR settlement prices for the Netherlands during the same time period were retrieved from Regelleistung.net (Regelleistung.net, 2022). During this time period, FCR auctions were still on a daily basis instead of on a 4-h basis. To account for this, it has been assumed that the FCR auction price (in €/MW/h) during each of the six 4-h auctions is the same as the daily auction price.

3.3.3 Grid frequency data

Frequency data from the French TSO, RTE France, is used in this analysis (RTE France, 2022). This data resembles the grid frequency in the Netherlands, as France is part of the same synchronous area (i.e., Continental Europe Synchronous Area). The original data is at a 10-s resolution. This data is resampled to 5 min by selecting the first frequency value of every 5-min interval to reduce the computational time while conserving a decent resolution.

3.3.4 Other data inputs

An overview of the remaining data inputs for the simulations is presented in Table 2. A 15-min modeling resolution was used for all simulations. An exception is the modeling of BEB charging in case of FCR market participation, which was modeled using a 5-min resolution to account for short-term frequency fluctuations and the short-term activation of reserves. Different bid prices for participation in the aFRR and FCR market were considered to show the impact of these bid prices on model outcomes. As discussed in Table 2, the reported aFRR bid prices are based on the difference between the aFRR market price and the day-ahead market price. The model simulations also considered different values of $P_{peak,max}$ when modeling aFRR and FCR participation, to find the optimal trade-off between grid tariffs and revenues from ancillary service participation for different maximum peak power values. This is outlined in Section 4.1.1.

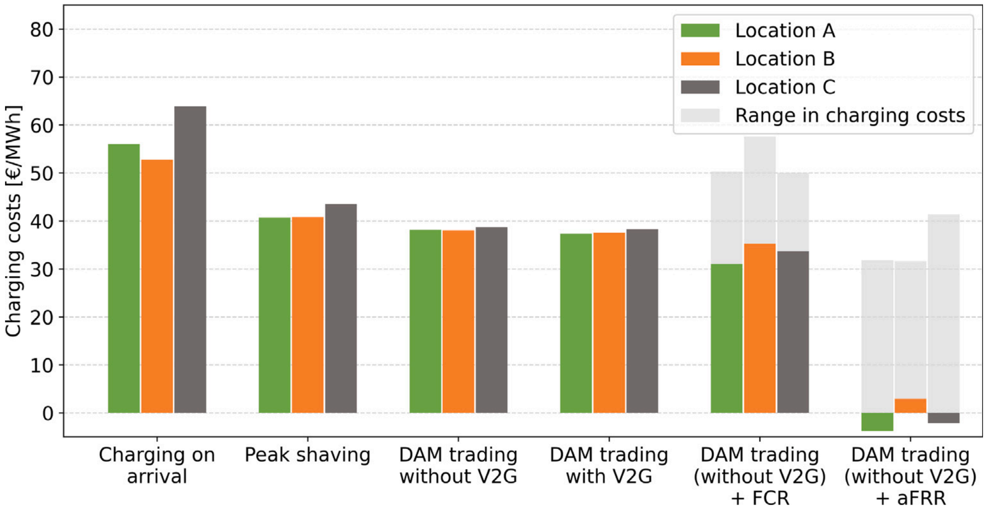

Fig. 2. Overview of charging costs for different locations and for different considered combinations of charging strategies. The charging costs comprise day-ahead market costs, grid tariffs, battery degradation costs and benefits in the ancillary service markets. For the strategies considering the provision of FCR and aFRR, the results are presented for the strategy (bid price, maximum charging power) resulting in the lowest charging costs. The range in charging costs for these strategies is presented in gray.

Table 3
Breakdown of charging costs per considered charging strategy for every considered location.

		Charging-on-arrival	Peak shaving	DAM trading without V2G	DAM trading with V2G	DAM trading (without V2G) + FCR	DAM trading (without V2G) + aFRR
Day-ahead charging costs [€/MWh]	Location A	34.6	31.1	28.2	27.8	27.0	25.6
	Location B	32.3	29.5	26.1	26.1	24.9	23.5
	Location C	35.7	29.4	24.4	25.3	22.8	24.4
Grid tariffs [€/MWh]	Location A	16.8	5.3	5.3	5.1	18.6	22.1
	Location B	15.6	6.6	7.1	6.7	10.4	16.4
	Location C	23.2	9.4	9.4	8.1	13.1	15.7
Battery degradation costs [€/MWh]	Location A	4.6	4.3	4.6	4.7	5.5	8.2
	Location B	4.9	4.7	4.9	4.9	5.2	5.9
	Location C	4.9	4.7	4.9	5.0	5.3	6.5
Ancillary service market benefits [€/MWh]	Location A	0.0	0.0	0.0	0.0	−20.1	−59.7
	Location B	0.0	0.0	0.0	0.0	−5.2	−42.8
	Location C	0.0	0.0	0.0	0.0	−7.5	−48.8
Total costs [€/MWh]	Location A	56.0	40.7	38.1	37.6	31.0	−3.8
	Location B	52.8	40.8	38.1	37.7	35.2	3.0
	Location C	63.9	43.5	38.7	38.4	33.7	−2.1

4 Results

4.1 Economic analysis

Fig. 2 presents a comparison of the BEB charging costs for the different considered combinations of charging strategies at the three studied locations. These costs comprise day-ahead market costs, grid tariffs, battery degradation costs and benefits in the ancillary service markets. A breakdown of these costs for each charging strategy at each location is presented in Table 3.

The charging cost reduction when shifting from charging-on-arrival to peak-shaving is substantial, ranging from 22.8–31.9% for different locations. This indicates that grid tariffs can have a considerable impact on overall charging costs and that adapting charging schedules to reduce the peak charging power results in considerable cost reductions. Participating in the day-ahead market can further reduce charging costs by 6.3–11.1% compared to the peak-shaving charging strategy. As indicated in Table 3, the grid fees at all locations stay the same or only increase marginally when shifting from the peak-shaving charging strategy to participation in the day-ahead electricity market. This indicates that it is not cost-efficient to increase the grid capacity and grid tariffs to create extra room for cost optimization in the day ahead market.

Using V2G to reduce BEB charging costs in the day-ahead market has limited effect compared to day-ahead market optimization without V2G, with a cost reduction of 0.8–1.4% compared to this charging strategy. First, this can be attributed to the extra efficiency losses and battery degradation costs with V2G, which cause the benefits of an extra charging/discharging cycle in many cases to not

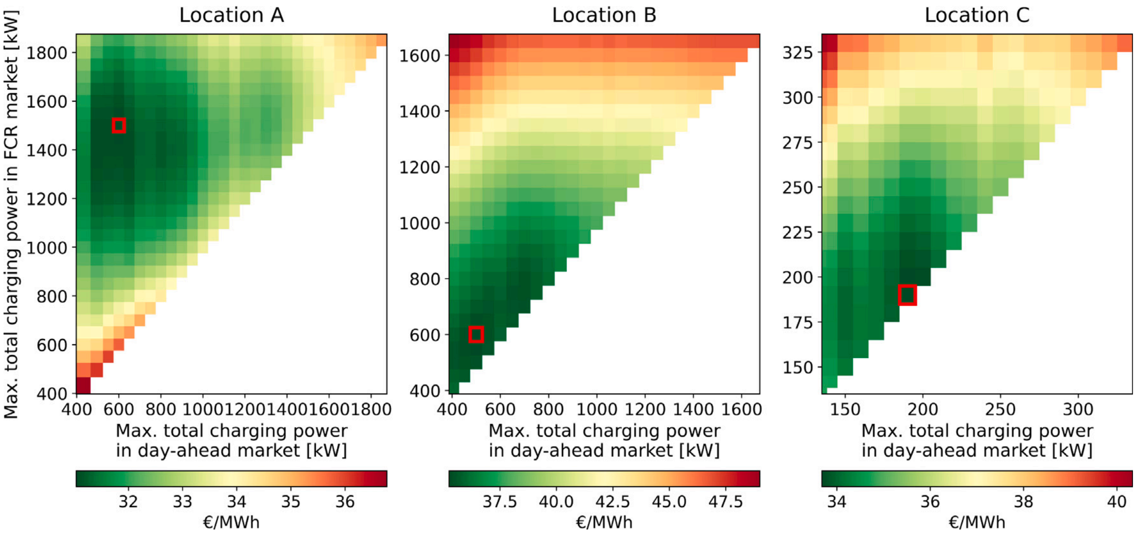

Fig. 3. Total charging costs for three considered locations when participating in the FCR market for different maximum peak power values in the day-ahead and in the FCR market. The combination with the lowest charging costs is highlighted using a red marker. This figure considered an FCR bid price of 0 €/MW/h.

outweigh the extra costs associated with such a cycle. Second, the complementarity between typical bus schedules and beneficial moments for discharging BEBs is low. Relatively high day-ahead market prices generally occur in the early evening and morning hours, during which BEBs arrive at the depot with relatively low SoC. This means that BEBs are mostly unavailable to discharge during moments characterized by relatively high electricity prices. Similarly, most buses depart from a depot before peak-demand hours associated with high electricity prices

There is high potential for charging cost reduction when participating in ancillary services markets. Participating in the FCR market can reduce charging costs by 6.6–17.5% compared to the DAM trading with V2G charging strategy when considering the optimal FCR bidding strategy. When participating in the aFRR market, overall charging costs can be reduced to below 0 €/MWh when considering the optimal aFRR bidding strategy. However, it should be noted that the range in charging costs in Fig. 2 for the FCR and aFRR bidding strategies indicates that a sub-optimal bidding strategy may result in an increase in charging costs compared to the other charging strategies. The optimal charging strategy in both ancillary service markets depends on the FCR and aFRR bid prices and the maximum peak charging power for charging in the day-ahead and FCR/aFRR market. Section 4.1.1 discusses the optimal BEB charging strategy for both the FCR and aFRR markets.

The considerably higher reduction in overall charging costs with aFRR market participation compared to FCR market participation can mostly be attributed to higher ancillary market revenues when participating in the aFRR market. This is due to the difference in market design between both markets. FCR bidding occurs for 4-h periods and FCR bids are symmetrical. Consequently, the full potential for the provision of FCR cannot be met at all time steps. In contrast, the full available upward and downward aFRR potential for each ISP can be offered to the aFRR market, Thus, more reserves can be offered to this market, resulting in higher revenues.

The slight differences in charging costs between locations are mostly induced by the connection hours of BEBs. The charging costs at Location C are highest with the charging-on-arrival or peak-shaving strategies, which is caused by a large concentration of BEBs arriving at the depot within a short time span, causing a high peak charging demand and high grid tariffs. At other depots, the arrival of BEBs is more evenly spread over a day, inducing lower charging demand peaks. The charging costs at Location C are equal or below the charging costs of other depots with other charging strategies. This indicates that the flexibility to charge at moments with beneficial electricity prices is higher at this depot.

4.1.1 Optimal bidding strategy in FCR and aFRR market

As outlined in Sections 2.3.1 and 2.3.2, the FCR and aFRR bid size can be constrained by a maximum peak power $P_{peak,max}$. A higher value of $P_{peak,max}$ increases grid tariffs but also provides more opportunities for bidding to the FCR and aFRR markets. If the peak charging power is increased for the provision of ancillary services, the maximum charging power that should be considered in the day-ahead market could also be fully or partially increased to reduce charging costs in the day-ahead market.

Fig. 3 provides insight in the total charging costs when participating in the FCR market with different combinations of $P_{peak,max}$ for the day-ahead and FCR market. For all investigated locations, the optimal combination with the lowest overall charging costs requires an increase in the peak charging power compared to day-ahead market optimization only, indicating that the extra FCR revenues that can be made in this case outweigh the higher grid tariffs. However, the optimal charging strategy differs between the considered locations. At the locations with a larger number of BEBs (Location A and B), the optimal value for $P_{peak,max}$ for the day-ahead market optimization is lower than the value of $P_{peak,max}$ for the FCR market, which means that some grid capacity is

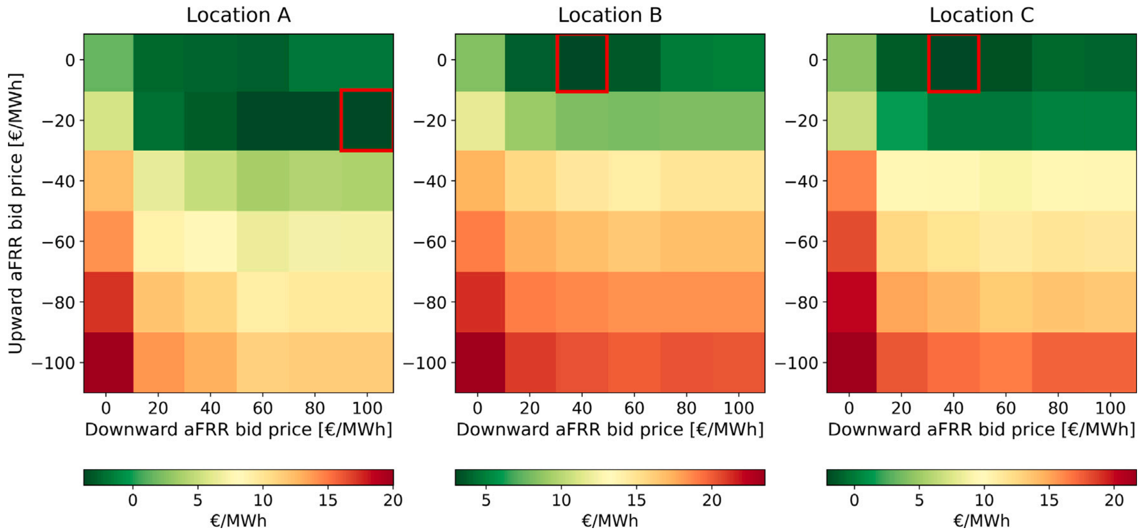

Fig. 4. Total charging costs for three considered locations when participating in the aFRR market for different upward and downward aFRR bid prices. The optimal combination of bid prices is highlighted using a red marker. The reported costs represent the lowest costs for the considered combination of bid prices. As explained in Section 3.3.4, the presented bid prices represent the difference between the day-ahead market price and the aFRR settlement prices.

reserved for the provision of FCR after day-ahead market optimization. Reserving grid capacity for FCR provision is cost-efficient due to the 4-h bidding period of the FCR market. If equal values of $P_{peak,max}$ are considered for day-ahead market optimization and FCR bidding, the FCR bid size during the full auction period is 0 kW if the BEB charging load from the day-ahead market optimization equals $P_{peak,max}$ during one moment of the auction period. Considering a higher value of $P_{peak,max}$ with FCR bidding makes sure that FCR bids are not restricted to 0 kW for a large share of FCR auctions. Reserving some grid capacity for the provision of FCR is less attractive at locations with a smaller fleet of BEBs, such as Location C, since the smaller bus fleet means that less often sufficient BEBs are connected to the charging stations for participation in the FCR auctions.

FCR revenues are highest when assuming a bid price of 0 €/MW/h to increase the chance of the bid being accepted, since marginal pricing is applied in this market, which means that all accepted market bids receive the same FCR settlement price. Increasing the FCR bid price considerably reduces the revenue in the FCR markets; an FCR bid price of 12 €/MW/h reduces the FCR revenues at Location A by 96% when considering the cost-optimal charging strategy.

Since the potential for BEBs to provide aFRR at a certain moment depends on previous aFRR activations, as explained in Section 2.3.2, low aFRR bid prices are not necessarily the cost-optimal bidding strategy at the aFRR market. The cost-optimal combination of bid prices for each considered location is presented in Fig. 4.

At all studied locations, the optimal downward aFRR bid price is lower than the optimal upward aFRR bid price. A BEB can only provide upward aFRR if it has provided downward aFRR earlier during the charging transaction. Therefore, a high downward aFRR bid price will cause that BEBs will have only very limited opportunities to provide upward aFRR, losing the opportunities to make aFRR bids at moments with beneficial prices.

The upward aFRR bid price should not be too low, since any activation of downward aFRR will shortly be followed by activation of upward aFRR. As a consequence, BEBs will not be able to make upward aFRR bids at moments with beneficial aFRR settlement prices. A high upward aFRR bid price can induce low aFRR activation volumes. The optimal upward aFRR bid price differs between locations, but overall differences in net charging costs are relatively small with different upward aFRR bid prices, as long as downward aFRR bid prices are low.

The optimal values of $P_{peak,max}$ when participating in the aFRR market are presented in Fig. 5. Also with aFRR market participation, it is beneficial to increase the peak charging power compared to the peak charging power with day-ahead market trading only, to be able to provide more aFRR reserves. For the locations with a larger BEB fleet (Locations A and B), it is not cost-efficient to reserve grid capacity for aFRR provision when optimizing the day-ahead schedules, in contrast to the optimal FCR bidding strategy, due to the shorter bidding period in the aFRR market. At Location C, the cost-optimal strategy is to reserve some grid capacity for aFRR market bidding, although the difference in charging costs when not reserving grid capacity for the aFRR market is marginal.

4.2 Grid impact analysis

The load duration curves presented in Fig. 6 provide insight into the impact of different BEB charging strategies on the grid for the different locations.

It is apparent that considering grid tariffs in the scheduling of BEBs directly reduces the grid impact of BEB charging; applying a peak-shaving algorithm reduces the peak load by 58–69% compared to the charging-on-arrival strategy. To avoid an increase in

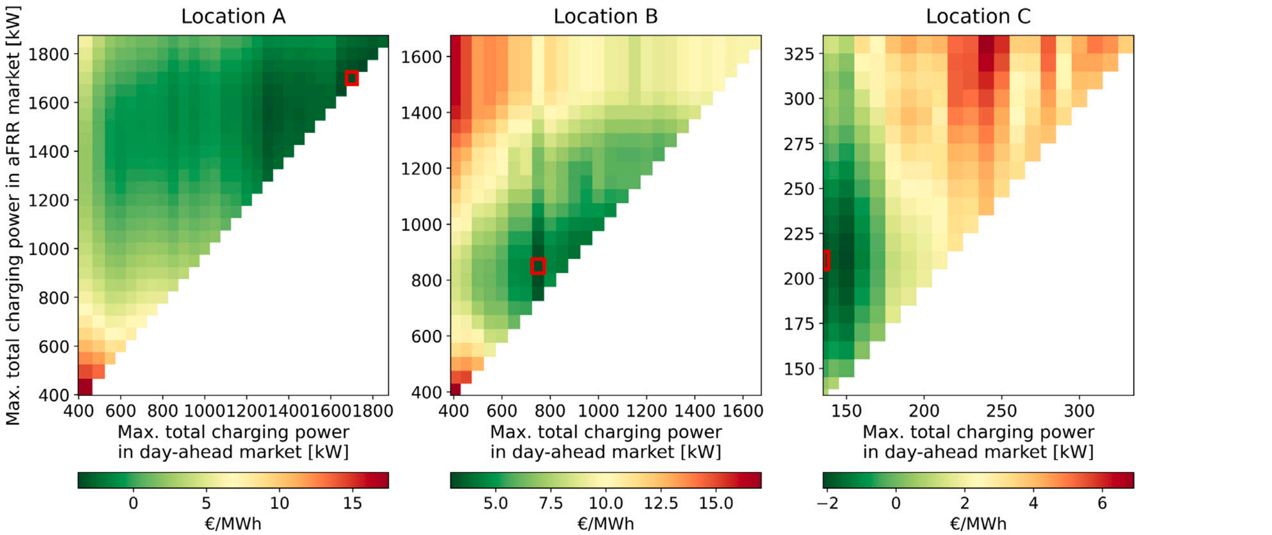

Fig. 5. Total charging costs for the three considered locations when participating in the aFRR market for different maximum peak power values in the day-ahead and in the aFRR market. The combination with the lowest charging costs is highlighted using a red marker. The considered aFRR bid prices are the optimal aFRR bid prices for the respective location.

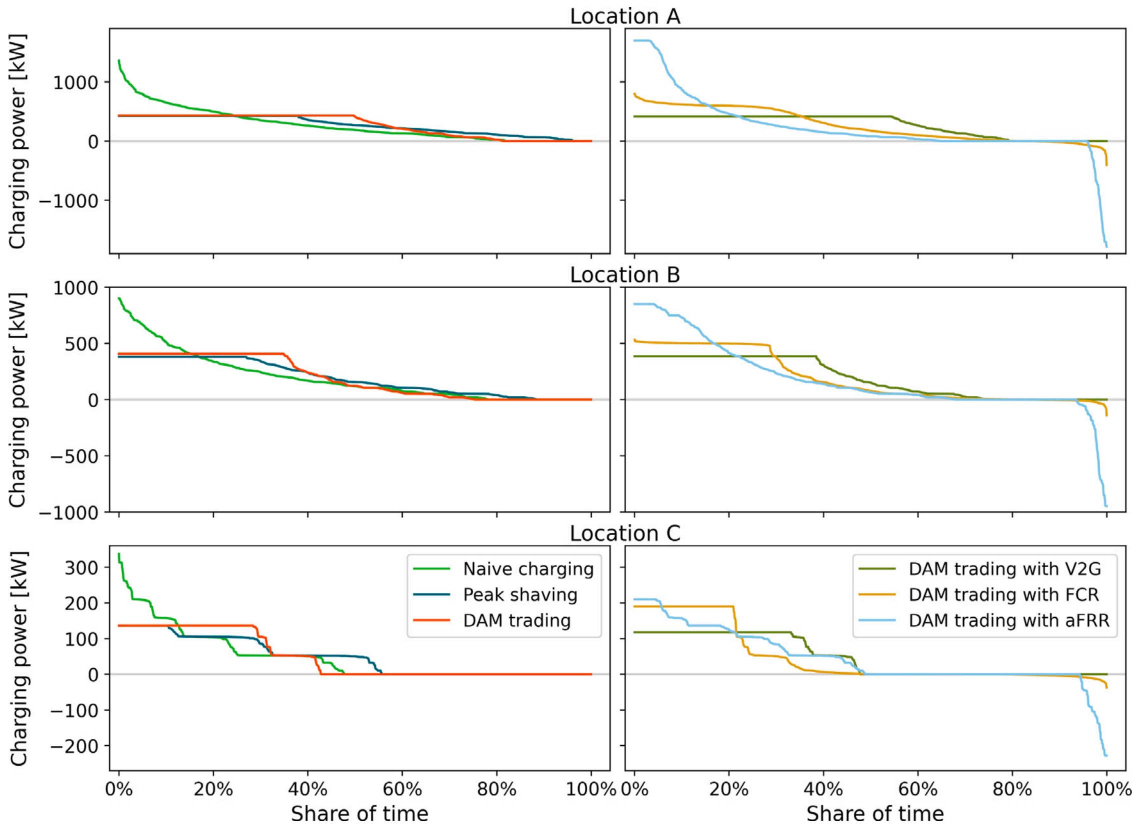

Fig. 6. Load duration curve for the considered charging strategies for the three considered locations. The load duration curve of the cost-optimal strategy is presented for the 'DAM with FCR' and 'DAM with aFRR' charging strategies.

grid fees, the peak load stays the same or increases only marginally compared to peak-shaving when also considering day-ahead market prices. It is also clear that the BEBs charge for a considerable share of time at the peak load value in both the peak-shaving and day-ahead market optimization charging strategies. At all considered locations, the share of time at which the BEBs charge at the peak load value is higher with the day-ahead market charging strategy compared to the peak-shaving strategy. Similarly, the share of time in which the charging power equals zero is also higher with the day-ahead market charging strategy. Both trends are caused by the fact that day-ahead prices are considered in the charging optimization; BEBs are charging at maximum power at moments with beneficial day-ahead prices, and are not charging when the prices are not beneficial.

The share of time at which the total charging power is negative with DAM trading with V2G is low, mainly due to the fact that the charging demand of BEBs should be met at departure and that it rarely happens that the extra efficiency losses and extra battery degradation costs of a discharging cycle are outweighed by the financial benefits of this cycle. However, this charging strategy provides the opportunity to reduce the total charging, since the charging demand of some BEBs can be fulfilled by the discharging of other BEBs. As discussed in Section 4.1, FCR and aFRR activation to resolve grid imbalances induces high peak demand, potentially causing stress on the local electricity grid. The increase in peak load is even higher when providing aFRR, since aFRR bids are fully activated upon acceptance, whereas the activation of FCR bids is relative to the frequency deviation and full FCR activation rarely occurs.

5 Discussion

This study assessed the economic and grid impact of different BEB charging strategies using model simulations with historical BEB charging data from three different locations. Different aspects should be considered when interpreting the results of this analysis.

The economic analysis in this research indicated that charging-on-arrival results in the highest costs and that considerable cost reductions are possible using peak-shaving or DAM trading. This is in line with the conclusions of previous studies looking at the cost reduction potential of electric vehicles (Li et al., 2020; Zheng et al., 2020). Participation in the FCR and aFRR markets can lead to further cost reductions. It should be noted that in a real-life application, each envisioned strategy will add costs and complexity to the daily operation of the bus operator. Participating in the day-ahead market causes that the BEB charging demand and availability is forecasted and that bids are made available to this market. Similarly, investments in specific hardware in BEBs and charging stations might be required to be able to provide V2G services using BEBs. Participating in ancillary services markets requires real-time optimization and adaptation of charging schedules. The increasing complexity of the daily operation of a bus operator could result in extra operational costs, which may outweigh the financial benefits of switching to the more-advanced charging strategy.

The peak-shaving and the day-ahead optimization models with and without V2G are deterministic, assuming a foreknown charging demand, arrival time, and departure time of BEBs. Hence, the results of this analysis provide insight into the theoretical cost-reduction potential of these charging strategies. Although the arrival times and departure times of BEBs are highly predictable due to the existence of bus timetables, delays in arrival cause that the number of BEBs charging at a depot cannot be predicted with absolute accuracy. Also, the electricity consumption of BEBs is not constant and is affected by different factors, including driver experience and weather conditions (Vepsäläinen et al., 2019; Gallet et al., 2018). Hence, the actual cost-reduction potential of these charging strategies might be slightly lower than presented in this work. Given the research and stakeholders' objectives, future work can detail further on the integration of uncertainty factors into the BEB charging models, for instance through stochastic optimization. In addition, future research could expand the proposed models with more-elaborate battery degradation models and with CC-CV (non-linear) charging characteristics. However, it should be considered that integrating these aspects into the models considerably increase their computational burden and that the outcome of the model simulations is dependent on the considered stochastic optimization technique.

It should also be highlighted that the outcomes of the model simulations cannot be generalized. These outcomes are the results of a case study and could differ considerably for other bus depots in other locations and with different charging characteristics of the BEB fleet. This study used electricity market prices from the beginning of 2020, which might not be representative of a future situation. Future electricity market prices can be influenced by the increasing adoption of RES, geopolitical conflicts and the electrification of the energy system, potentially affecting the financial attractiveness of considering these markets in the BEB scheduling process.

One of the main findings of this study is that participating in the aFRR market can reduce charging costs to almost 0 €/MWh. No perfect foresight of aFRR prices was assumed when modeling participation in this market; activation of aFRR was only based on the aFRR bid price and the aFRR market price at that specific moment, and future aFRR prices were not considered. Hence, it might be possible to achieve results close to this theoretical cost reduction potential in practice. The optimal bidding strategy in this study was determined ex-post and cannot be determined ex-ante. However, an analysis using historical price data, similar to the analysis conducted in this study, can support in determining the optimal bidding strategy in the future.

Two relevant aspects of the investigated case study should be considered. Grid tariffs are based on the annual peak load, but the analysis timeframe in this research is considerably shorter than one year. Although a correction factor has been applied to the grid tariffs, the annual peak load could be different than the reported peak loads in this analysis. Similarly, this study considered the same auction price for all 4-h FCR auctions during the day, since 4-h auctions were not yet implemented during the considered assessment timeframe in this study. In practice, there will be price variability between the different auctions during a day (ENTSO-E, 2022). Both aspects could affect the exact model outcomes, however, it is unlikely that the overall trends in the results will be affected.

The results of this analysis have different implications for bus operators and grid operators. Since the results indicate that the potential cost savings when implementing different smart charging algorithms are very high, bus operators need to pay attention to the fueling process of their buses, whereas this required little attention with conventional combustion-engine buses. Therefore, bus operators need to make investments in data management and data analysis to optimize the scheduling of BEBs. In addition, bus operators should look into collaborations with Balance Responsible Parties (BRPs) in order to get access to the electricity markets.

The grid impact of different BEB charging strategies has direct implications for grid operators. High BEB charging peaks can induce congestion at the local grid level, or at higher levels. Grid operators need to consider this when making future projections of grid congestion and power quality problems in low and medium-voltage grids, and if necessary, act by reinforcing the grid. However, the results of this analysis indicate that BEBs can reduce their local grid impact by using a peak shaving strategy, which can help grid operators to defer grid investments. Also, the results indicate that BEBs can contribute to restoring system balance through the provision of FCR or aFRR, which means that less conventional power plants are required for the provision of these grid services.

6 Conclusion

This paper presented a novel framework for modeling different BEB charging strategies: charging-on-arrival, peak-shaving, DAM trading without V2G, DAM trading with V2G and participation in the FCR and aFRR ancillary services markets. The economic and grid impact of the different BEB charging strategies were analyzed by performing model simulations using a case study with input from historical BEB charging data of three depots of Dutch bus operator Qbuzz. Results indicate that applying smart charging to BEBs can considerably reduce BEB charging costs. Applying a peak-shaving algorithm reduces charging costs by 23–32% compared to the charging-on-arrival strategy. Optimizing day-ahead charging costs can further reduce BEB charging costs by 6–11% compared to the peak-shaving strategy. The results also indicated that BEBs can play a significant role in the provision of FCR and aFRR balancing reserves. The provision of these ancillary services can lead to considerable charging cost reductions; the charging costs reduction compared to the charging-on-arrival strategy with the optimal bidding strategy in the FCR market ranges between 33–47%, while the charging cost reduction with the optimal bidding strategy in the aFRR market ranges between 90–>100%. The optimal bidding strategy to the ancillary services markets differs per considered market and depends on the total number of BEBs in a depot and their availability during the day. In all cases, it is economically efficient to increase the grid capacity to be able to offer higher FCR and aFRR volumes to the market.

The grid impact analysis indicates that full electrification of a bus fleet can result in high BEB charging peaks, in particular if a charging-on-arrival strategy is applied to BEBs. This could potentially induce grid congestion problems. The grid impact of BEB charging is considerably lower when applying peak-shaving or DAM trading charging strategies, due to the damping effect of grid tariffs on BEB charging peaks. Participating in the FCR or aFRR market increases the BEB peak charging power compared to peak-shaving or DAM trading charging algorithms.

Overall, BEB smart charging results in major cost reductions and should seriously be considered by bus operators. Applying a peak-shaving strategy is the lowest-hanging fruit for bus operators and leads to considerable cost reductions. Day-ahead market optimization, the use of V2G and bidding in the FCR market can further reduce charging costs to a limited extent, but the implementation of these charging strategies adds complexity to integration and operation. Although the implementation of the aFRR charging strategy is also complex, it should be considered by bus operators due to the high potential cost reductions that can be achieved.

CRediT authorship contribution statement

Nico Brinkel: Conceptualization, Methodology, Software, Formal analysis, Writing – original draft, Writing – review & editing, Visualization. **Marle Zijlstra:** Conceptualization, Methodology, Software, Formal analysis, Writing – original draft, Visualization. **Ronald van Bezu:** Conceptualization, Data curation, Writing – review & editing, Supervision. **Tim van Twuijver:** Conceptualization, Writing – review & editing, Supervision. **Ioannis Lampropoulos:** Conceptualization, Writing – review & editing, Supervision. **Wilfried van Sark:** Conceptualization, Writing – review & editing, Supervision, Funding acquisition.

Appendix. Background information on the considered electricity and ancillary services markets

This section provides background information on the functioning and structure of the considered electricity and ancillary services markets.

A.1. Day-ahead market

The day-ahead market is the electricity market with the highest trading volumes in Europe (EPEX Spot, 2022). This market consists of daily auctions, to which market participants can make supply and demand bids for every hour of the next day. Every bid consists of a bidding volume and a bid price. Market bids should be made before the gate-closure time of 12:00, after which the market is cleared. From the market clearing process follows the day-ahead price for every bidding zone for every hour of the next day. The day-ahead price is based on the demand and supply bid curves of different bidding zones and the available cross-border capacity between bidding zones. All market bids with a supply bid price below or equal to the day-ahead price or a demand bid price above or equal to the day-ahead price are accepted. Marginal pricing is used in this market, meaning that all accepted market bids pay/receive the same price.

A.2. FCR market

To avoid frequency deviations in the electricity grid, the demand and supply of electricity should continuously be balanced. If a market participant deviates from its accepted day-ahead market bid, imbalance occurs. TSOs activate reserves to restore the grid balance. FCR, also referred to as primary reserves, are activated first. Activation of FCR happens automatically based on the frequency fluctuations throughout Europe, and energy resources providing FCR should be able to be fully activated within 30 s after the frequency fluctuation (ENTSO-E, 2022).

FCR capacity is contracted in every bidding zone to assure sufficient FCR capacity is available. This happens through auctions. Any market participant that is contracted in an auction should be able to provide the bidded FCR capacity during the full auction period (Lampropoulos et al., 2018). As of July 2020, the duration of one auction period has changed from 24 h to 4 h. FCR is a symmetrical product, meaning that the FCR provider must be able to both provide upward FCR (i.e., decrease in consumption or an increase in generation) or downward FCR (i.e., decrease in generation or an increase in consumption) during the bidding period. All FCR market bids with a bid price equal or below the resulting FCR auction price are contracted. In case their FCR market bids are contracted, market participants receive the FCR auction price as a financial compensation for providing FCR capacity. The market participants do not receive financial compensation for activation of FCR. This study only considered indivisible market bids, meaning that the bidded capacity is always fully accepted or rejected. In practice, also divisible market bids are possible.

A.3. aFRR market

In case of sustained imbalance, aFRR is activated to assure the FCR capacity is available to respond in case of a future imbalance event. aFRR resources should be able to be fully operational within 5 min after being activated (TenneT TSO, 2022).

Market participants can provide aFRR in different ways (Lampropoulos et al., 2018). First, TSOs need to contract a minimum aFRR capacity. Contracted aFRR resources receive financial compensation and are obliged to offer aFRR to the market during the whole bidding period. Second, market participants can offer aFRR capacity for one or multiple 15-min imbalance settlement periods (ISPs) without being contracted. This is the only method that is considered in this study. Third, market participants can deliberately deviate from their day-ahead market bid without explicitly offering capacity to the aFRR auction. This mechanism is often referred to as ‘passive balancing’.

FCR is an asymmetrical product, meaning that market participants can separately offer upward and downward aFRR capacity. For every ISP, the TSO sorts both the upward and downward aFRR bids based on their bid price, without distinguishing between contracted and non-contracted bids. In case of an imbalance event, aFRR activation happens using the merit order, meaning that the aFRR market bids with the lowest bid price are activated first in case of upward aFRR, and the bids with highest bid price are activated first with downward aFRR.

The aFRR price depends on the activated aFRR volumes. Generally, the aFRR price is equal to the highest activated aFRR upward bid or lowest aFRR downward bid. All activated aFRR reserves and all market participants deviating from their day-ahead market bid pay this price in case of extra consumption, or receive this price in case of extra generation.

References

Bagherinezhad, A., Palomino, A.D., Li, B., Parvania, M., 2020. Spatio-temporal electric bus charging optimization with transit network constraints. IEEE Trans. Ind. Appl. (ISSN: 19399367) 56 (5), 5741–5749. http://dx.doi.org/10.1109/TIA.2020.2979132.

Brinkel, N., Schram, W., AlSkaif, T., Lampropoulos, I., van Sark, W., 2020. Should we reinforce the grid? Cost and emission optimization of electric vehicle charging under different transformer limits. Appl. Energy (ISSN: 0306-2619) 276 (October), 115285. http://dx.doi.org/10.1016/j.apenergy.2020.115285.

Broos, P., Ockers, M., Van Rookhuyzen, J., 2017. Marktverkenning Elektrische bussen (Market Exploration for Electric Buses). Tech. Rep., ElaadNL, pp. 1–47, [Online]. Available: https://www.elaad.nl/uploads/downloads/downloads_download/ElaadNL_Marktverkenning_Elektrische_Bussen_november_2017.pdf.

CBS Statline, 2019. Emissions to air on dutch territory; road traffic. [Online]. Available: https://opendata.cbs.nl/#/CBS/en/dataset/7063eng/table?ts=1626687398080.

Chen, H., Hu, Z., Xu, Z., Li, J., Zhang, H., Xia, X., Ning, K., Peng, M., 2016. Coordinated charging strategies for electric bus fast charging stations. In: Asia-Pacific Power and Energy Engineering Conference, APPEEC, Vol. 2016-December. pp. 1174–1179. http://dx.doi.org/10.1109/APPEEC.2016.7779677, no. 51477082, ISSN : 21574847.

ENTSO-E, 2019. Automatic Frequency Restoration Reserve Process - Implementation Guide. Tech. Rep., [Online]. Available: https://docstore.entsoe.eu/Documents/EDI/Library/ERRP/Automatic_Frequency_Restoration_Reserve_Process_IG_v1.0.pdf.

ENTSO-E, 2021. Network code - frequency containment reserves (FCR). [Online]. Available: https://www.entsoe.eu/network_codes/eb/fcr/.

ENTSO-E, 2022. ENTSO-E Transparency Platform. [Online]. Available: https://transparency.entsoe.eu/.

ENTSO-E, 2022. Frequency containment reserves (FCR). [Online]. Available: https://www.entsoe.eu/network_codes/eb/fcr/.

EPEX Spot, 2022. Basics of the power market. [Online]. Available: https://www.epexspot.com/en/basicspowermarket.

European Environmental Agency, 2018. National emissions reported to the UNFCCC and to the EU greenhouse gas monitoring mechanism. [Online]. Available: https://www.eea.europa.eu/data-and-maps/data/national-emissions-reported-to-the-unfccc-and-to-the-eu-greenhouse-gas-monitoring-mechanism-17.

European Union Agency for the Cooperation of Energy Regulators, 2021. ACER Report on Distribution Tariff Methodologies in Europe. Tech. Rep., p. 88.

Gallet, M., Massier, T., Hamacher, T., 2018. Estimation of the energy demand of electric buses based on real-world data for large-scale public transport networks. Appl. Energy (ISSN: 03062619) 230 (August), 344–356. http://dx.doi.org/10.1016/j.apenergy.2018.08.086.

Gao, Y., Guo, S., Ren, J., Zhao, Z., Ehsan, A., Zheng, Y., 2018. An electric bus power consumption model and optimization of charging scheduling concerning multi-external factors. Energies (ISSN: 19961073) 11 (8), http://dx.doi.org/10.3390/en11082060.

Grijalva, E.R., López Martínez, J.M., 2019. Analysis of the reduction of CO2 emissions in urban environments by replacing conventional city buses by electric bus fleets: Spain case study. Energies (ISSN: 19961073) 12 (3), http://dx.doi.org/10.3390/en12030525.

Gurobi, 2022.

Houbbadi, A., Redondo-Iglesias, E., Trigui, R., Pelissier, S., Bouton, T., 2019. Optimal charging strategy to minimize electricity cost and prolong battery life of electric bus fleet. In: 2019 IEEE Vehicle Power and Propulsion Conference, VPPC 2019 - Proceedings. pp. 1–6. http://dx.doi.org/10.1109/VPPC46532.2019.8952493, no. October.

Interprovincial Consultation, Dutch Ministry of Infrastructure and Environment, Metropole region Rotterdam/The Hague, Transport region Amsterdam, 2016. Bestuursakkoord Zero Emissie Regionaal Openbaar Vervoer Per Bus (Administrative Agreement on Zero-Emission Regional Public Bus Transport). Tech. Rep., [Online]. Available: https://www.greendeals.nl/sites/default/files/uploads/2015/04/Bestuursakkoord_Zero_OV-Bus_v3.pdf.

Jahic, A., Eskander, M., Schulz, D., 2019. Charging schedule for load peak minimization on large-scale electric bus depots. Appl. Sci. (Switzerland) (ISSN: 20763417) 9 (9), http://dx.doi.org/10.3390/app9091748.

Kennisplatform CROW, 2020. Staat van het OV 2019 (current state of public transport 2019). [Online]. Available: https://www.crow.nl/staat-van-het-ov/jaargangen/2019.

Lago, J., De Ridder, F., Vrancx, P., De Schutter, B., 2018. Forecasting day-ahead electricity prices in europe: The importance of considering market integration. Appl. Energy (ISSN: 03062619) 211 (December 2017), 890–903. http://dx.doi.org/10.1016/j.apenergy.2017.11.098, arXiv:1708.07061.

Lajunen, A., Lipman, T., 2016. Lifecycle cost assessment and carbon dioxide emissions of diesel, natural gas, hybrid electric, fuel cell hybrid and electric transit buses. Energy (ISSN: 03605442) 106, 329–342. http://dx.doi.org/10.1016/j.energy.2016.03.075.

Lampropoulos, I., van den Broek, M., van der Hoofd, E., Hommes, K., van Sark, W., 2018. A system perspective to the deployment of flexibility through aggregator companies in the netherlands. Energy Policy (ISSN: 03014215) 118 (February), 534–551. http://dx.doi.org/10.1016/j.enpol.2018.03.073.

Lampropoulos, I., Gort, S., Brinkel, N., Van Sark, W., 2022. Charging strategies for electric buses based on deterministic and stochastic optimisation approaches: A dutch case study. In: 26th International Conference and Exhibition on Electricity Distribution.

Leou, R.C., Hung, J.J., 2017. Optimal charging schedule planning and economic analysis for electric bus charging stations. Energies (ISSN: 19961073) 10 (4), http://dx.doi.org/10.3390/en10040483.

Li, X., Tan, Y., Liu, X., Liao, Q., Sun, B., Cao, G., Li, C., Yang, X., Wang, Z., 2020. A cost-benefit analysis of V2G electric vehicles supporting peak shaving in Shanghai. Electr. Power Syst. Res. (ISSN: 03787796) 179 (October 2019), 106058. http://dx.doi.org/10.1016/j.epsr.2019.106058.

Lymperopoulos, I., Qureshi, F.A., Bitlislioglu, A., Poland, J., Zanarini, A., Mercangoez, M., Jones, C., 2020. Ancillary services provision utilizing a network of fast-charging stations for electrical buses. IEEE Trans. Smart Grid (ISSN: 19493061) 11 (1), 665–672. http://dx.doi.org/10.1109/TSG.2019.2927701.

Manzolli, J.A., Trovão, J.P.F., Henggeler Antunes, C., 2022. Electric bus coordinated charging strategy considering V2G and battery degradation. Energy (ISSN: 03605442) 254, http://dx.doi.org/10.1016/j.energy.2022.124252.

Moradipari, A., Tucker, N., Zhang, T., Cezar, G., Alizadeh, M., 2020. Mobility-aware smart charging of electric bus fleets. IEEE Power Energy Soc. Gen. Meet. (ISSN: 19449933) 2020-August, http://dx.doi.org/10.1109/PESGM41954.2020.9281897, arXiv:1912.05681.

Münderlein, J., Steinhoff, M., Zurmühlen, S., Sauer, D.U., 2019. Analysis and evaluation of operations strategies based on a large scale 5 MW and 5 MWh battery storage system. J. Energy Storage (ISSN: 2352152X) 24 (April), http://dx.doi.org/10.1016/j.est.2019.100778.

Python Software Foundation, 2022. Python Language Reference. [Online]. Available: https://docs.python.org/3/reference/.

Qin, N., Gusrialdi, A., Paul Brooker, R., T-Raissi, A., 2016. Numerical analysis of electric bus fast charging strategies for demand charge reduction. Transp. Res. A (ISSN: 09658564) 94, 386–396. http://dx.doi.org/10.1016/j.tra.2016.09.014.

Raab, A.F., Lauth, E., Strunz, K., Göhlich, D., 2019. Implementation schemes for electric bus fleets at depots with optimized energy procurements in virtual power plant operations. World Electr. Veh. J. (ISSN: 20326653) 10 (1), 1–14. http://dx.doi.org/10.3390/wevj10010005.

Regelleistung.net, 2022. Data Center. [Online]. Available: https://www.regelleistung.net/apps/datacenter/tenders/.

Rinaldi, M., Parisi, F., Laskaris, G., D'Ariano, A., Viti, F., 2018. Optimal dispatching of electric and hybrid buses subject to scheduling and charging constraints. In: IEEE Conference on Intelligent Transportation Systems, Proceedings, ITSC, Vol. 2018-November. pp. 41–46. http://dx.doi.org/10.1109/ITSC.2018.8569706.

Rogge, M., van der Hurk, E., Larsen, A., Sauer, D.U., 2018. Electric bus fleet size and mix problem with optimization of charging infrastructure. Appl. Energy (ISSN: 03062619) 211 (November 2017), 282–295. http://dx.doi.org/10.1016/j.apenergy.2017.11.051.

RTE France, 2022. RTE Customer's area - Network frequency. [Online]. Available: http://clients.rte-france.com/lang/an/visiteurs/vie/vie_frequence.jsp.

Rupp, M., Rieke, C., Handschuh, N., Kuperjans, I., 2020. Economic and ecological optimization of electric bus charging considering variable electricity prices and CO2eq intensities. Transp. Res. D (ISSN: 13619209) 81 (March), 102293. http://dx.doi.org/10.1016/j.trd.2020.102293.

Sassi, O., Cherif, W.R., Oulamara, A., 2015. Vehicle routing problem with mixed fleet of conventional and heterogenous electric vehicles and time dependent charging costs. Int. J. Math., Comput., Phys., Electr. Comput. Eng. 9 (3), 167–177, [Online]. Available: https://hal.archives-ouvertes.fr/hal-01083966/%0Ahttp://waset.org/Publication/vehicle-routing-problem-with-mixed-fleet-of-conventional-and-heterogenous-electric-vehicles-and-time-dependent-charging-costs/10000760.

Schram, W., Brinkel, N., Smink, G., Van Wijk, T., Van Sark, W., 2020. Empirical evaluation of V2G round-trip efficiency. In: SEST 2020 - 3rd International Conference on Smart Energy Systems and Technologies. http://dx.doi.org/10.1109/SEST48500.2020.9203459.

Steber, D., Pruckner, M., Bazan, P., German, R., 2017. SWARM - providing 1 MW FCR power with residential PV-battery energy storage - simulation and empiric validation. 2017 IEEE Manch. PowerTech, Powertech 2017 http://dx.doi.org/10.1109/PTC.2017.7981091.

Stedin DSO, 2019. Elektriciteit - Tarieven 2019 (Electricity - Tariffs 2019). Tech. Rep., pp. 26–28.

Stroe, D.I., Knap, V., Swierczynski, M., Stroe, A.I., Teodorescu, R., 2017. Operation of a grid-connected lithium-ion battery energy storage system for primary frequency regulation: A battery lifetime perspective. IEEE Trans. Ind. Appl. (ISSN: 00939994) 53 (1), 430–438. http://dx.doi.org/10.1109/TIA.2016.2616319.

Stumpe, M., Röß ler, D., Schryen, G., Kliewer, N., 2021. Study on sensitivity of electric bus systems under simultaneous optimization of charging infrastructure and vehicle schedules. EURO J. Transp. Logist. (ISSN: 21924384) 10 (January), 100049. http://dx.doi.org/10.1016/j.ejtl.2021.100049.

Swierczynski, M., Stroe, D.I., Stan, A.I., Teodorescu, R., Kaer, S.K., 2015. Lifetime estimation of the nanophosphate LiFePO4 battery chemistry used in fully electric vehicles. IEEE Trans. Ind. Appl. (ISSN: 00939994) 51 (4), 3453–3461. http://dx.doi.org/10.1109/TIA.2015.2405500.

TenneT TSO, 2022. Handboek aFRR voor BSPs (aFRR Manual for BSPs). Tech. Rep., [Online]. Available: https://netztransparenz.tennet.eu/fileadmin/user_upload/SO_NL/Handboek_aFRR_voor_BSPs.pdf.

Vas-Corrales, A., Nguyen, P., Vergara, P.P., Schoot, W., Söder, L., 2021. Framework to evaluate power portfolio dispatch considering balancing market participation. In: 2021 IEEE Madrid PowerTech. pp. 1–6.

Vepsäläinen, J., Otto, K., Lajunen, A., Tammi, K., 2019. Computationally efficient model for energy demand prediction of electric city bus in varying operating conditions. Energy (ISSN: 03605442) 169, 433–443. http://dx.doi.org/10.1016/j.energy.2018.12.064.

Wang, S., Fernandez, C., Chunmei, Y., Yongcun, F., Wen, C., Stroe, D., Chen, Z., 2021. Battery System Modeling. Elsevier.

Wang, Y., Huang, Y., Xu, J., Barclay, N., 2017. Optimal recharging scheduling for urban electric buses: A case study in Davis. Transp. Res. E (ISSN: 13665545) 100, 115–132. http://dx.doi.org/10.1016/j.tre.2017.01.001.

Zhang, L., Wang, S., Qu, X., 2021. Optimal electric bus fleet scheduling considering battery degradation and non-linear charging profile. Transp. Res. E (ISSN: 13665545) 154 (April), 102445. http://dx.doi.org/10.1016/j.tre.2021.102445.

Zhang, Y.J.A., Zhao, C., Tang, W., Low, S.H., 2018. Profit-maximizing planning and control of battery energy storage systems for primary frequency control. IEEE Trans. Smart Grid (ISSN: 19493053) 9 (2), 712–723. http://dx.doi.org/10.1109/TSG.2016.2562672, arXiv:1604.00952.

Zheng, Y., Yu, H., Shao, Z., Jian, L., 2020. Day-ahead bidding strategy for electric vehicle aggregator enabling multiple agent modes in uncertain electricity markets. Appl. Energy (ISSN: 03062619) 280 (September), 115977. http://dx.doi.org/10.1016/j.apenergy.2020.115977.

Zhou, B., Wu, Y., Zhou, B., Wang, R., Ke, W., Zhang, S., Hao, J., 2016. Real-world performance of battery electric buses and their life-cycle benefits with respect to energy consumption and carbon dioxide emissions. Energy (ISSN: 03605442) 96 (2016), 603–613. http://dx.doi.org/10.1016/j.energy.2015.12.041.